NOAA Technical Memorandum
NWS ER-88

A SYNOPTIC AND MESOSCALE EXAMINATION OF THE NORTHERN NEW ENGLAND WINTER STORM OF 29-30 JANUARY 1990

ROBERT A MARINE
STEVEN J. CAPRIOLA

National Weather Service Forecast Office
Portland, Maine

Scientific Services Division
Eastern Region Headquarters
Bohemia, New York
July, 1994

U.S. DEPARTMENT OF COMMERCE
National Oceanic and Atmospheric Administration
National Weather Service

NOAA TECHNICAL MEMORANDA
National Weather Service, Eastern Region Subseries

The National Weather Service Eastern Region (ER) Subseries provides an informal medium for the documentation and quick dissemination of results not appropriate, or not yet ready for formal publications. The series is used to report on work in progress, to describe technical procedures and practices, or to relate progress to a limited audience. These Technical Memoranda will report on investigations devoted primarily to regional and local problems of interest mainly to ER personnel, and usually will not be widely distributed.

Papers 1 to 22 are in the former series, ESSA Technical Memoranda, Eastern Region Technical Memoranda (ERTM); papers 23 to 37 are in the former series, ESSA Technical Memoranda, Weather Bureau Technical Memoranda (WBTM). Beginning with 38, the papers are now part of the series, NOAA Technical Memoranda NWS.

Papers 1 to 22 are available from the National Weather Service Eastern Region, Scientific Services Division, 630 Johnson Avenue, Bohemia, NY 11716. Beginning with 23, the papers are available from the National Technical Information Service, U.S. Department of Commerce, Sills Bldg., 5285 Port Royal Road, Springfield, VA 22161. Prices vary for paper copy and for microfiche. Order by accession number shown in parentheses at end of each entry.

ESSA Technical Memoranda

ERTM 1 Local Uses of Vorticity Prognoses in Weather Prediction. Carlos R. Dunn. April 1965.
ERTM 2 Application of the Barotropic Vorticity Prognostic Field to the Surface Forecast Problem. Silvio G. Simplicio. July 1965.
ERTM 3 A Technique for Deriving an Objective Precipitation Forecast Scheme for Columbus, Ohio. Robert Kuessner. September 1965.
ERTM 4 Stepwise Procedures for Developing Objective Aids for Forecasting the Probability of Precipitation. Carlos R. Dunn. November 1965.
ERTM 5 A Comparative Verification of 300 mb. Winds and Temperatures Based on NMC Computer Products Before and After Manual Processing. Silvio G. Simplicio. March 1966.
ERTM 6 Evaluation of OFDEV Technical Note No. 17. Richard M. DeAngelis. March 1966.
ERTM 7 Verification of Probability of Forecasts at Hartford, Connecticut, for the Period 1963-1965. Robert B. Wassall. March 1966.
ERTM 8 Forest-Fire Pollution Episode in West Virginia, November 8-12, 1964. Robert O. Woodfall. April 1966.
ERTM 9 The Utilization of Radar in Meso-Scale Synoptic Analysis and Forecasting. Jerry D. Hill. March 1966.
ERTM 10 Preliminary Evaluation of Probability of Precipitation Experiment. Carlos R. Dunn. May 1966.
ERTM 11 Final Report. A Comparative Verification of 300 mb. Winds and Temperatures Based on NMC Computer Products Before and After Manual Processing. Silvio G. Simplicio. May 1966.
ERTM 12 Summary of Scientific Services Division Development Work in Sub-Synoptic Scale Analysis and Prediction - Fiscal Year 1966. Fred L. Zuckerberg.
ERTM 13 A Survey of the Role of Non-Adiabatic Heating and Cooling in Relation of the Development of Mid-Latitude Synoptic Systems. Constantine Zois. July 1966.
ERTM 14 The Forecasting of Extratropical Onshore Gales at the Virginia Capes. Glen V. Sachse. August 1966.
ERTM 15 Solar Radiation and Clover Temperatures. Alex J. Kish. September 1966.
ERTM 16 The Effects of Dams, Reservoirs and Levees on River Forecasting. Richard M. Greening. September 1966.
ERTM 17 Use of Reflectivity Measurements and Reflectivity Profiles for Determining Severe Storms. Robert E. Hamilton. October 1966.
ERTM 18 Procedure for Developing a Nomograph for Use in Forecasting Phenological Events from Growing Degree Days. John C. Purvis and Milton Brown. December 1966.
ERTM 19 Snowfall Statistics for Williamsport, Pa. Jack Hummel. January 1967.
ERTM 20 Forecasting Maturity Date of Snap Beans in South Carolina. Alex J. Kish. March 1967.
ERTM 21 New England Coastal Fog. Richard Fay. April 1967.
ERTM 22 Rainfall Probability at Five Stations Near Pickens, South Carolina, 1957-1963. John C. Purvis. April 1967.
WBTM ER 23 A Study of the Effect of Sea Surface Temperature on the Areal Distribution of Radar Detected Precipitation Over the South Carolina Coastal Waters. Edward Paquet. June 1967. (PB-180-612).
WBTM ER 24 An Example of Radar as a Tool in Forecasting Tidal Flooding. Edward P. Johnson. August 1967 (PB-180-613).
WBTM ER 25 Average Mixing Depths and Transport Wind Speeds over Eastern United States in 1965. Marvin E. Miller. August 1967. (PB-180-614).
WBTM ER 26 The Sleet Bright Band. Donald Marier. October 1967. (PB-180-615).
WBTM ER 27 A Study of Areas of Maximum Echo Tops in the Washington, D.C. Area During the Spring and Fall Months. Marie D. Fellechner. April 1968. (PB-179-339).
WBTM ER 28 Washington Metropolitan Area Precipitation and Temperature Patterns. C.A. Woollum and N.L. Canfield. June 1968. (PB-179-340).
WBTM ER 29 Climatological Regime of Rainfall Associated with Hurricanes after Landfall. Robert W. Schoner. June 1968. (PB-179-341).
WBTM ER 30 Monthly Precipitation - Amount Probabilities for Selected Stations in Virginia. M.H. Bailey. June 1968. (PB-179-342).
WBTM ER 31 A Study of the Areal Distribution of Radar Detected Precipitation at Charleston, S.C. S.K. Parrish and M.A. Lopez. October 1968. (PB-180-480).
WBTM ER 32 The Meteorological and Hydrological Aspects of the May 1968 New Jersey Floods. Albert S. Kachic and William Long. February 1969. (Revised July 1970). (PB-194-222).
WBTM ER 33 A Climatology of Weather that Affects Prescribed Burning Operations at Columbia, South Carolina. S.E. Wasserman and J.D. Kanupp. December 1968. (COM-71-00194).
WBTM ER 34 A Review of Use of Radar in Detection of Tornadoes and Hail. R.E. Hamilton. December 1969. (PB-188-315).
WBTM ER 35 Objective Forecasts of Precipitation Using PE Model Output. Stanley E. Wasserman. July 1970. (PB-193-378).
WBTM ER 36 Summary of Radar Echoes in 1967 Near Buffalo, N.Y. Richard K. Sheffield. September 1970. (COM-71-00310).
WBTM ER 37 Objective Mesoscale Temperature Forecasts. Joseph P. Sobel. September 1970. (COM-71-0074).

NOAA Technical Memoranda NWS

NWS ER 38 Use of Primitive Equation Model Output to Forecast Winter Precipitation in the Northeast Coastal Sections of the United States. Stanley E. Wasserman and Harvey Rosenblum. December 1970. (COM-71-00138).
NWS ER 39 A Preliminary Climatology of Air Quality in Ohio. Marvin E. Miller. January 1971. (COM-71-00204).
NWS ER 40 Use of Detailed Radar Intensity Data in Mesoscale Surface Analysis. Robert E. Hamilton. March 1971. (COM-71-00573).
NWS ER 41 A Relationship Between Snow Accumulation and Snow Intensity as Determined from Visibility. Stanley E. Wasserman and Daniel J. Monte. (COM-71-00763).
NWS ER 42 A Case Study of Radar Determined Rainfall as Compared to Rain Gage Measurements. Martin Ross. July 1971. (COM-71-00897).
NWS ER 43 Snow Squalls in the Lee of Lake Erie and Lake Ontario. Jerry D. Hill. August 1971. (COM-72-00959).
NWS ER 44 Forecasting Precipitation Type at Greer, South Carolina. John C. Purvis. December 1971. (COM-72-10332).
NWS ER 45 Forecasting Type of Precipitation. Stanley E. Wasserman. January 1972. (COM-72-10316).

(CONTINUED ON INSIDE REAR COVER)

NOAA Technical Memorandum NWS ER-88

A SYNOPTIC AND MESOSCALE EXAMINATION OF THE NORTHERN NEW ENGLAND WINTER STORM OF 29-30 JANUARY 1990

ROBERT A. MARINE
STEVEN J. CAPRIOLA

National Weather Service Forecast Office
Portland, Maine

Scientific Services Division
Eastern Region Headquarters
Bohemia, New York
July 1994

United States
Department of Commerce
Ronald H. Brown
Secretary

National Oceanic and
Atmospheric Administration
D. James Baker
Under Secretary

National Weather Service
Elbert W. Friday, Jr.
Assistant Administrator

TABLE OF CONTENTS

	PAGE
1. INTRODUCTION	1
2. SYNOPTIC OVERVIEW	1
2A. Surface Features	1
2B. Upper Air Features	4
2C. Precipitation	9
3. OTHER METEOROLOGICAL CONSIDERATIONS	12
3A. The Coastal Front	12
3B. Jet Streaks	12
3C. Evaporational Cooling	13
3D. Orographically Enhanced Precipitation	16
4. NATIONAL METEOROLOGICAL CENTER (NMC) MODEL PERFORMANCE	18
4A. Surface and Upper Air Forecasts	18
4B. Quantitative Precipitation Forecasts (QPF)	21
5. APPLICATIONS OF NMC GUIDANCE	25
5A. Precipitation Type	25
5B. The Meteorological "Bomb" Checklist	27
5C. The "Magic Chart"	31
6. SOME EMPIRICAL RULES FOR WINTER STORMS	34
7. FUTURE CONSIDERATIONS	37
8. CONCLUSIONS	37
REFERENCES	38

1. INTRODUCTION

On 29-30 January 1990, a low pressure system tracked parallel to the New England coastline and produced up to 20 inches of snow over portions of Maine, New Hampshire, and Vermont (Fig. 1). This detailed study will examine the large and small scale features that led to this heavy snow event. In addition, the use of various local forecast techniques and "rules of thumb" will be shown to be an effective way to improve upon dynamical model forecasts.

2. SYNOPTIC OVERVIEW

The development and path of the surface and upper air features were typical of many east coast snowstorms (Kocin and Uccellini 1990). A primary surface low tracked from the Tennessee River Valley northeast into western Pennsylvania. A secondary low developed on the warm front over southern Virginia and intensified rapidly as it tracked north along a coastal front to Cape Cod, then across the Gulf of Maine into Nova Scotia. At 500 mb, a short-wave trough moved from the lower Mississippi River Valley northeast into the Tennessee River Valley, and intensified as it lifted northeast across the Middle Atlantic States and southern New England. The precipitation pattern was also very common for heavy snow events in the Northeast. Snow spread rapidly from south to north in a broad warm advection, overrunning pattern. The snow mixed with ice pellets and changed to freezing rain across southern and coastal areas of Maine and New Hampshire, but remained all snow elsewhere, where total accumulations ranged from 12-20 in. A more detailed look at the surface, upper air, and precipitation patterns follows.

2A. Surface Features

At 1200 UTC 29 January 1990, surface high pressure (1028 mb) was centered in the Gulf of Maine just south of Nova Scotia with a ridge line extending northwest to James Bay (Fig. 2). At this time, a primary surface low was forming over the Tennessee Valley. During the next 12 hours, the high built to 1031 mb and drifted eastward, while the ridge line remained aligned to the northwest into southeast Canada. The surface low tracked northeastward into the central Appalachians and slowly deepened down to 1001 mb (Fig. 3). Southeast boundary layer winds increased over the northeastern United States as the pressure gradient tightened between these two systems.

The first indication of a coastal trough was evident at 0000 UTC 30 January (Fig. 4), as the wind direction at Nantucket, MA (ACK), and Atlantic City, NJ (ACY), became southeasterly, while the winds reported at Boston, MA (BOS), and Hartford, CT (BDL), were easterly and northerly, respectively. A temperature discontinuity was also evident with readings of 50°F at Atlantic City, 40°F at Nantucket, 36°F at Boston, and 34°F at Hartford. This developing coastal trough extended well north of a secondary surface low (1000 mb) that was forming in Virginia, in an area of large pressure falls (6 mb 3 h^{-1}). Note that the 0000 UTC 30 January Limited-area Fine Mesh (LFM) analysis (Fig. 3) depicts a single low center over northern Virginia, while the manual surface analysis (Fig. 4) clearly shows two distinct centers, representing the primary low over western Pennsylvania and a developing secondary low over

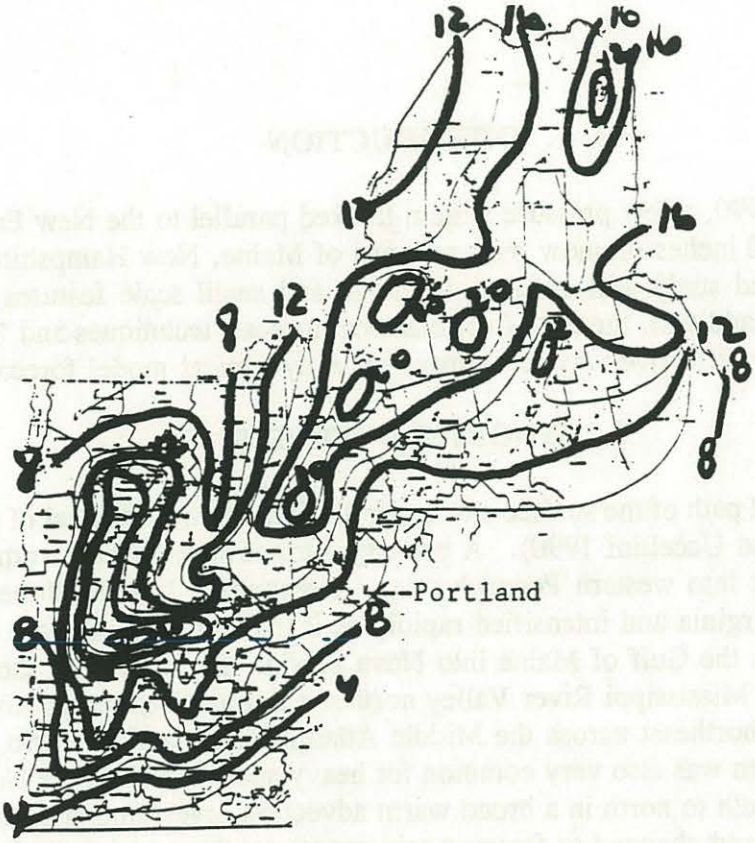

Figure 1. Storm-total snowfall (in) in New England for the snowstorm of 29-30 January 1990; contours are every two in (enhanced every four in).

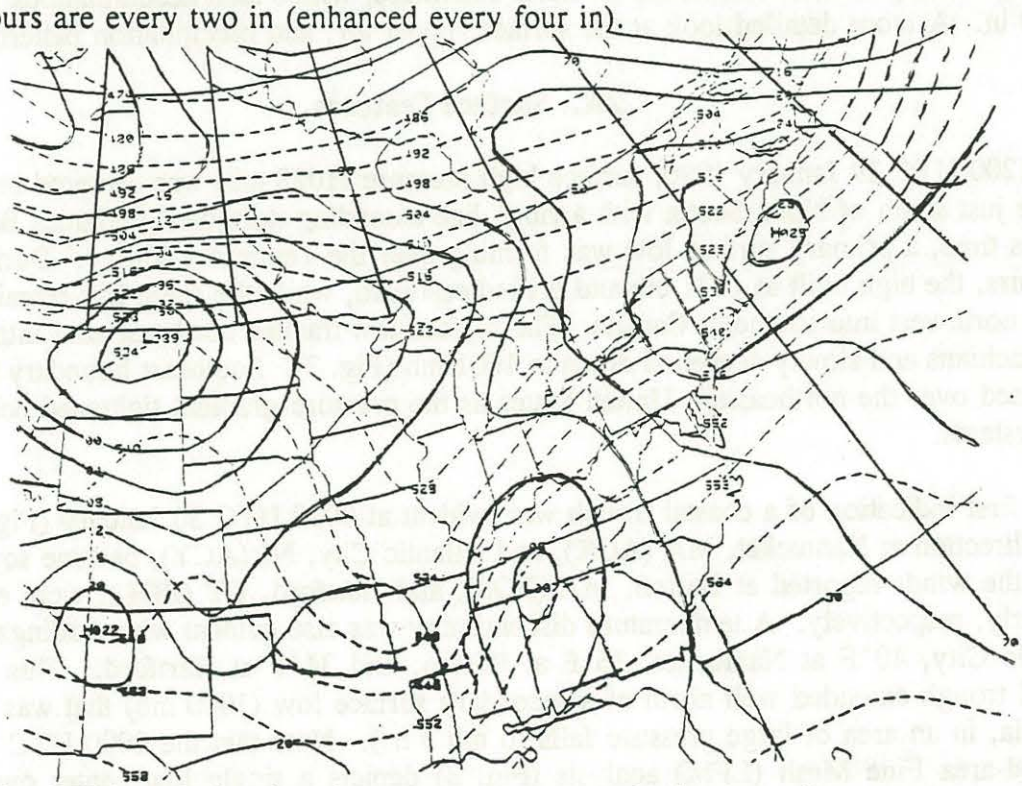

Figure 2. LFM analysis of surface pressure (mb; solid lines), surface pressure centers, and 1000-500 mb thickness (dm; dashed lines) for 1200 UTC 29 January 1990.

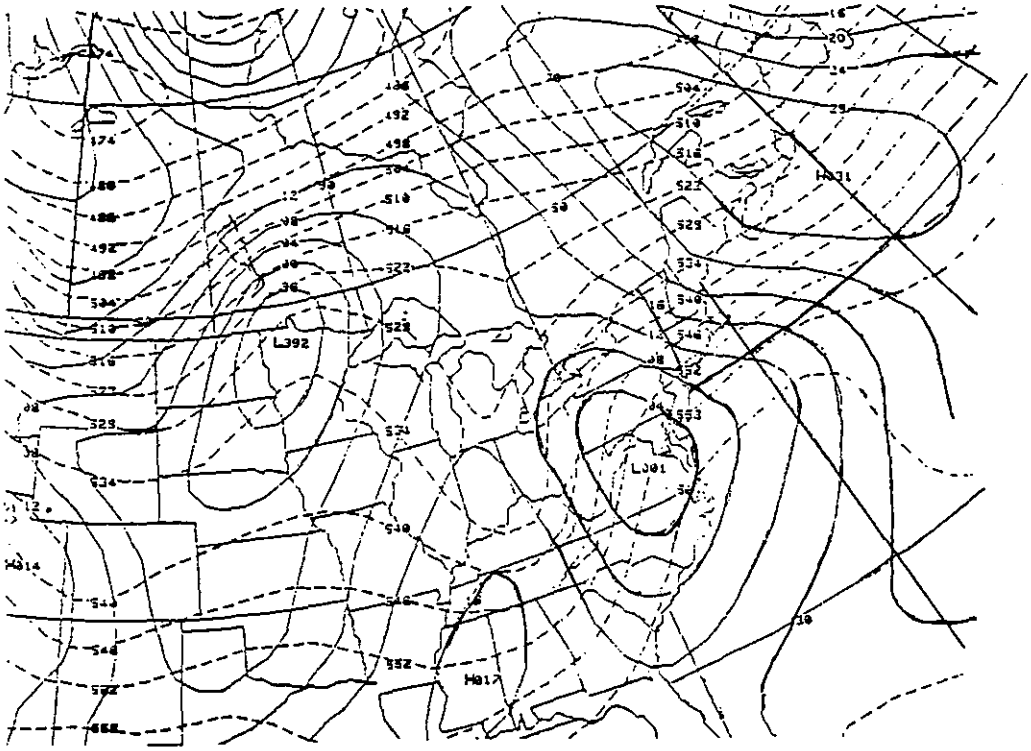

Figure 3. As in Figure 2, except for 0000 UTC 30 January 1990.

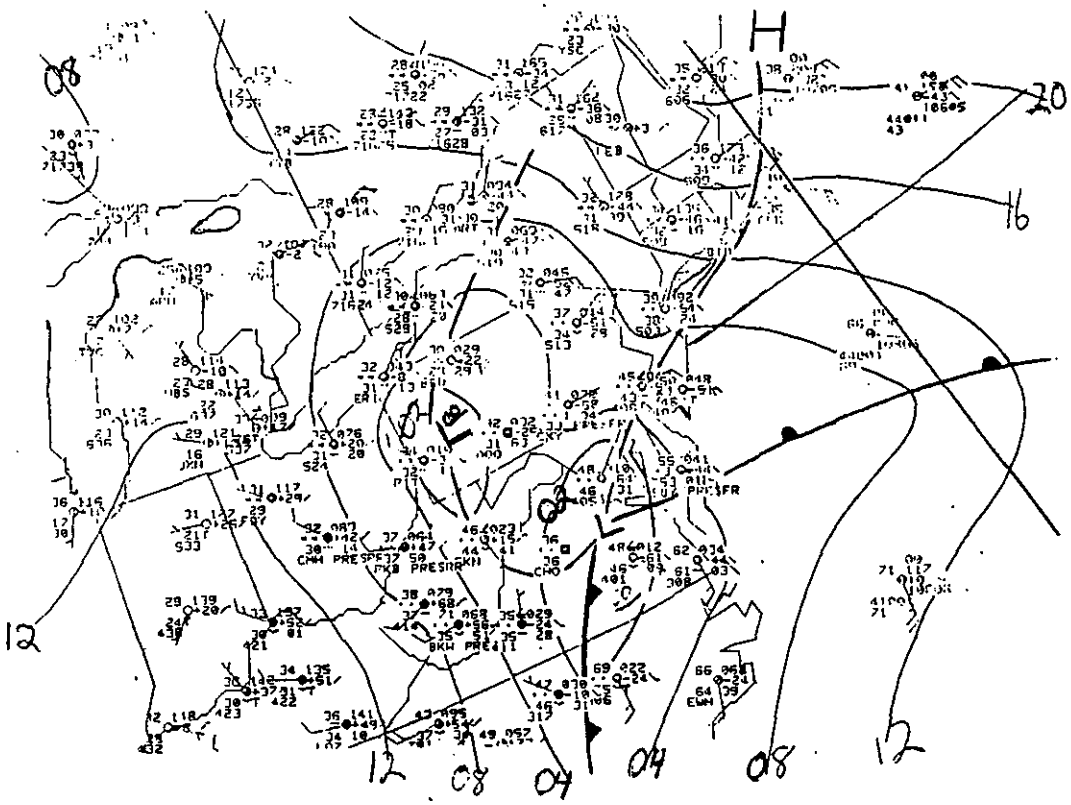

Figure 4. Surface data plot and meso-analysis for 0000 UTC 30 January 1990. Conventional representations used for surface features.

Virginia. This demonstrates the importance of doing a hand analysis and not relying solely on objective analyses. In general, the surface pattern fits the description of a category A storm as defined by Bosart (1975).

By 0600 UTC 30 January (Fig. 5), the secondary low had moved north along the coast to a position just south of New York City, and had deepened to 992 mb, while the original low moved into eastern Pennsylvania and began to be absorbed by the coastal low. In advance of the intensifying coastal storm, pressure falls approaching 10 mb 3 h^{-1} were observed in southern New England. Farther north, the surface ridge line remained across northern New England, while the coastal front cut across Cape Cod, MA, and extended northeast near Caches Ledge Buoy (44005) and Yarmouth, NS (YQI). The winds at Portland, ME (PWM), and Boston backed to the northeast as the coastal front strengthened, although by this time, temperatures had risen above freezing (33°F and 37°F, respectively), and the precipitation had changed to ice pellets at Portland. The low-level inflow was peaking around this time, as shown in the boundary layer geostrophic wind plot (Fig. 6), with maximum speeds approaching 65 kt from the east along the central Maine coast, and buoy reports indicated surface wind gusts were in excess of 50 kt. At 1200 UTC 30 January, the storm had consolidated into one center over the Gulf of Maine and continued to intensify down to 990 mb (Fig. 7). Figure 8 depicts the track of the coastal storm from south of Cape Cod at 0900 UTC 30 January (990 mb), to a position along the central Maine coast at 1600 UTC (983 mb). Thereafter, the low continued to deepen and accelerate northeastward towards Nova Scotia.

2B. Upper Air Features

A broad long-wave trough was located over the eastern United States during the period preceding the storm, while a ridge built over the western Atlantic and maintained a broad southwest flow aloft from the Gulf of Mexico into southern New England. A strong 500-mb short-wave trough intensified as it moved into the long wave position and eventually separated from the mean flow as a wind speed maximum, greater than 80 kt, dug across east Texas. The associated vorticity maximum (20×10^{-5} s^{-1}) was located in northern Arkansas at 1200 UTC 29 January (Fig. 9). Note that the LFM analysis, with 10-20 m errors in Missouri, Arkansas, and Illinois, does not capture the strength of the short-wave trough. This is another example of the importance of closely examining the data and doing hand analyses.

A deep layer of moisture, with dew point depressions under 6°C, is shown on the 500, 700, and 850 mb data plots (Figs. 9, 10, 11), from the central Gulf Coast northward into New England. Temperatures at 850 mb were cold across the Northeast, -10°C at Albany, NY (ALB), and -7°C at Portland. The 0°C isotherm extended from the Ohio Valley eastward to the southern New Jersey coast and well south of Long Island.

By 0000 UTC 30 January, the vorticity maximum (20×10^{-5} s^{-1}) was located just west of Huntington, WV (HTS), with a jet streak, exceeding 70 kt, from Athens, GA (AHN), to Atlantic City in the southeast quadrant of the 500-mb trough (Fig. 12). Abundant moisture extended through all levels of the troposphere ahead of the trough axis, except in extreme northern New

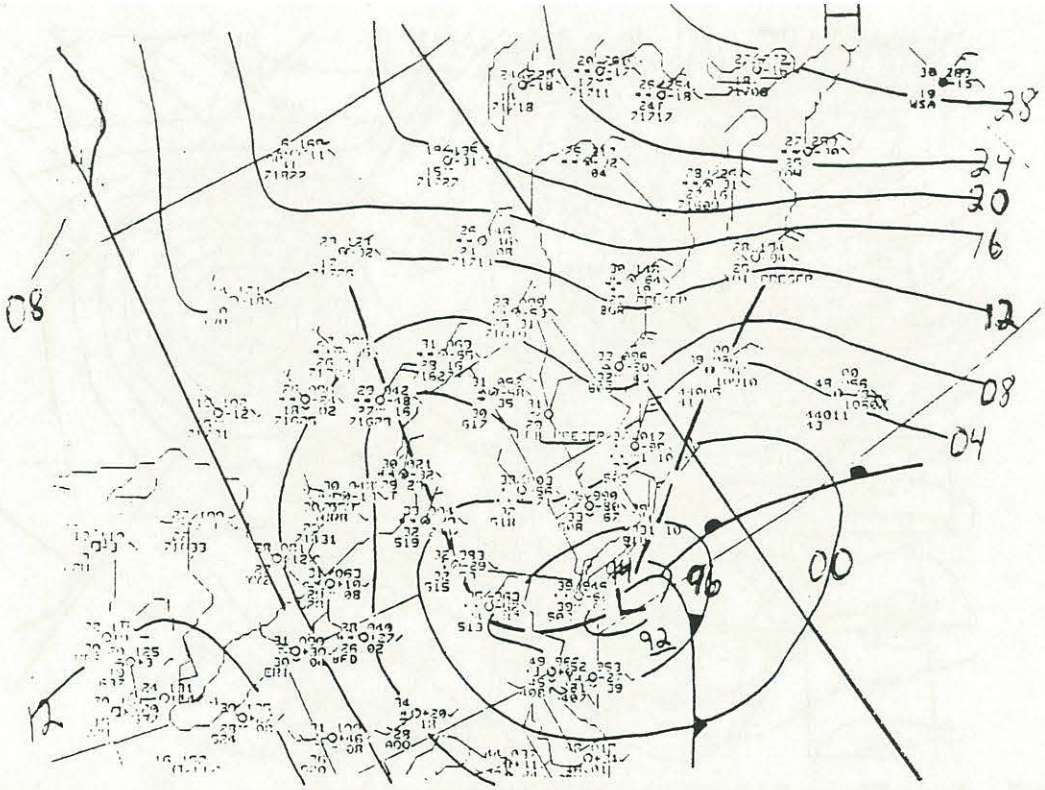

Figure 5. As in Figure 4, except for 0600 UTC 30 January 1990.

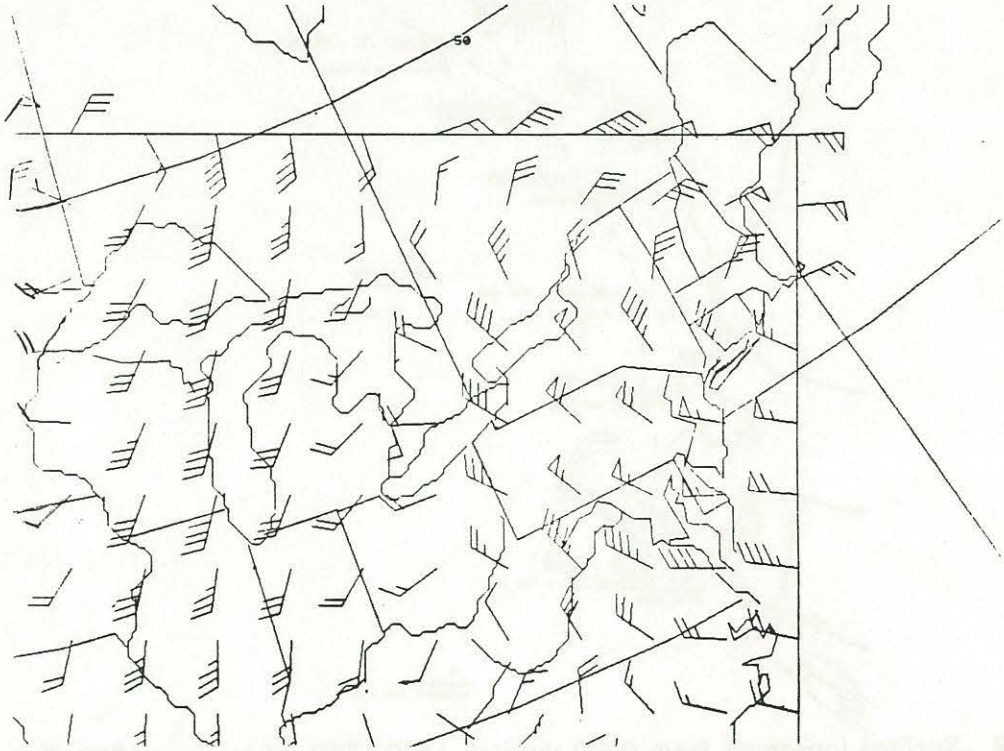

Figure 6. Geostrophic winds (kt; AFOS graphic 9AM) for 0900 UTC 30 January 1990.

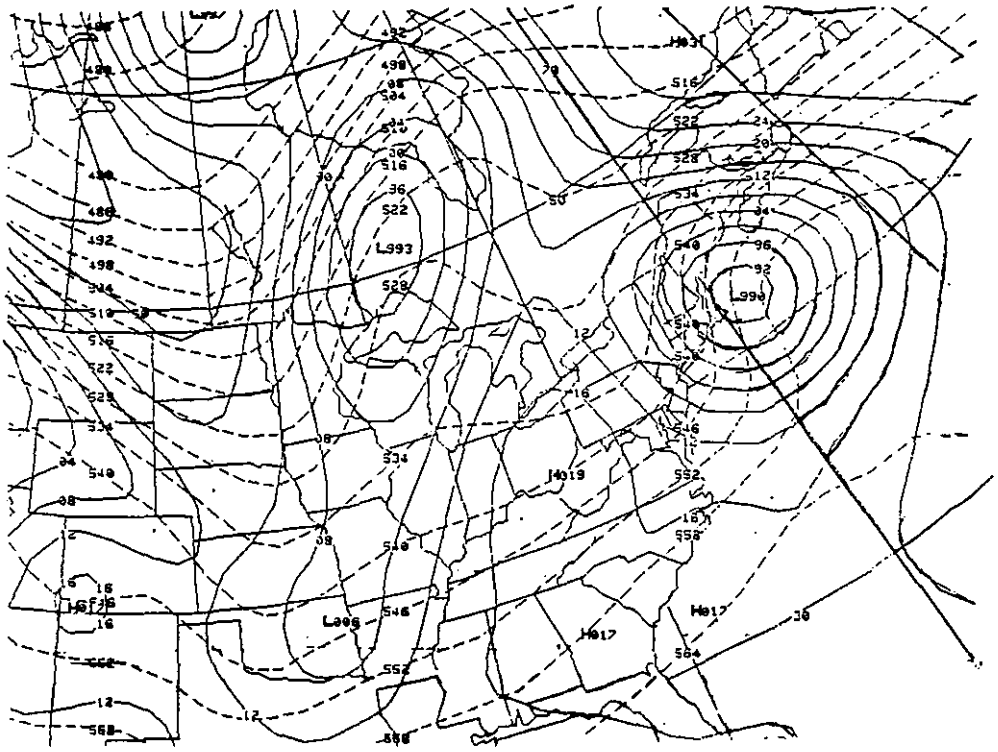

Figure 7. As in Figure 2, except for 1200 UTC 30 January 1990.

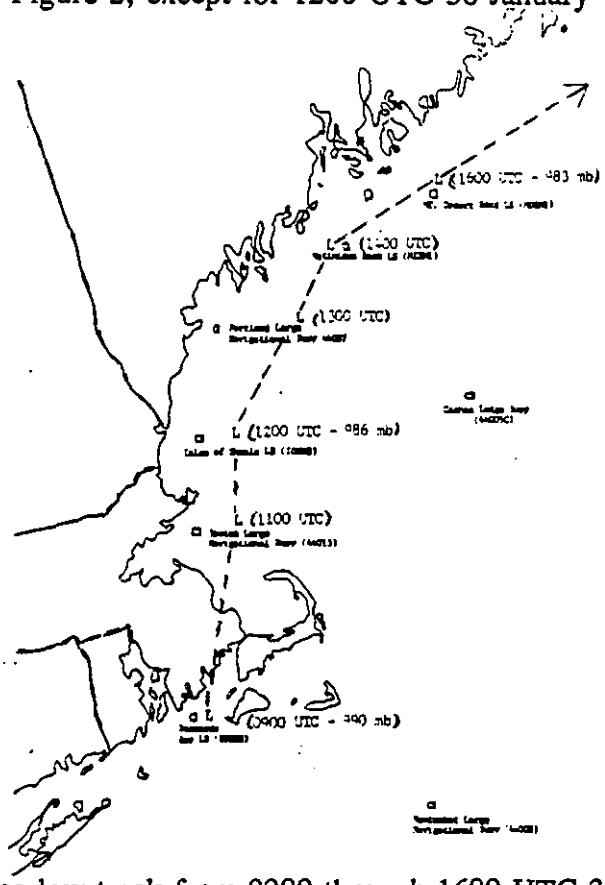

Figure 8. Surface low track from 0900 through 1600 UTC 30 January 1990; buoy identifiers are shown.

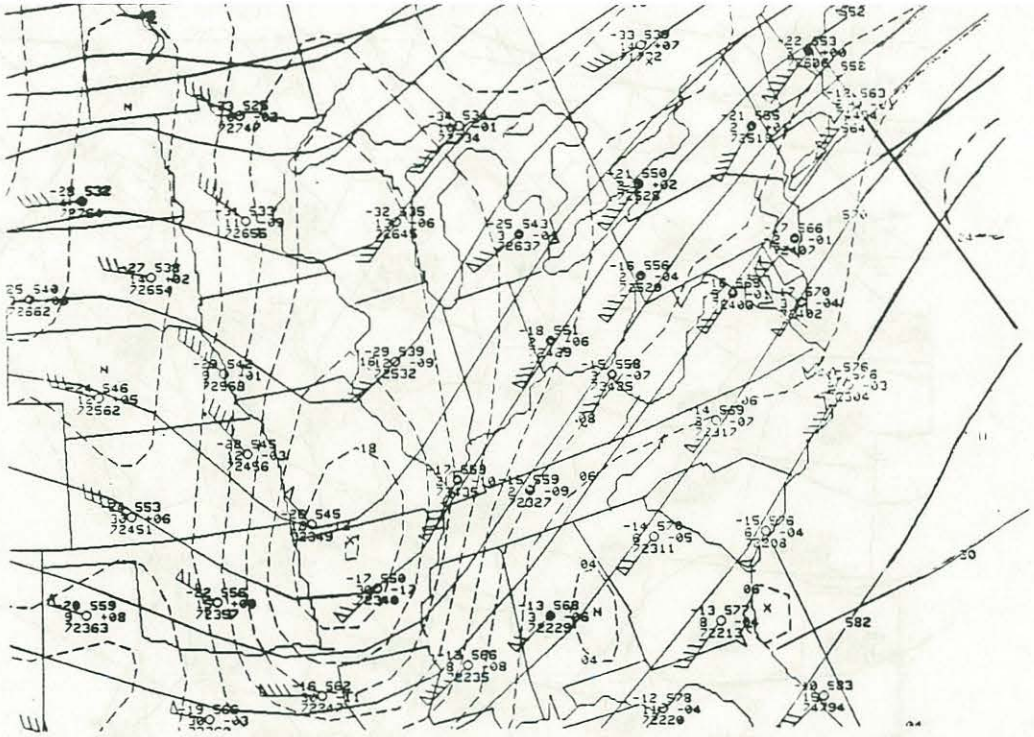

Figure 9. LFM 500-mb height (dm; solid lines) and vorticity (10^{-5} s^{-1}; dashed lines) analyses for 1200 UTC 29 January 1990. Standard notation is used for station models; dew point depressions ≤ 5°C are shaded.

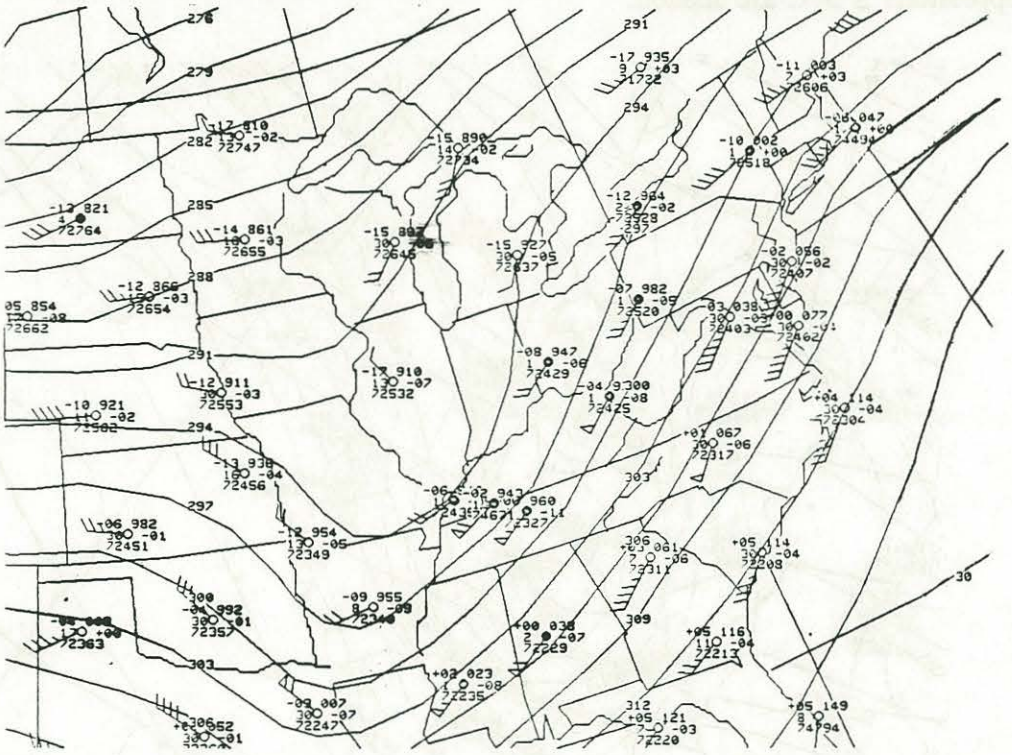

Figure 10. NGM 700-mb height (dm) analysis for 1200 UTC 29 January 1990. Standard notation is used for station models; dew point depressions ≤ 5°C are shaded.

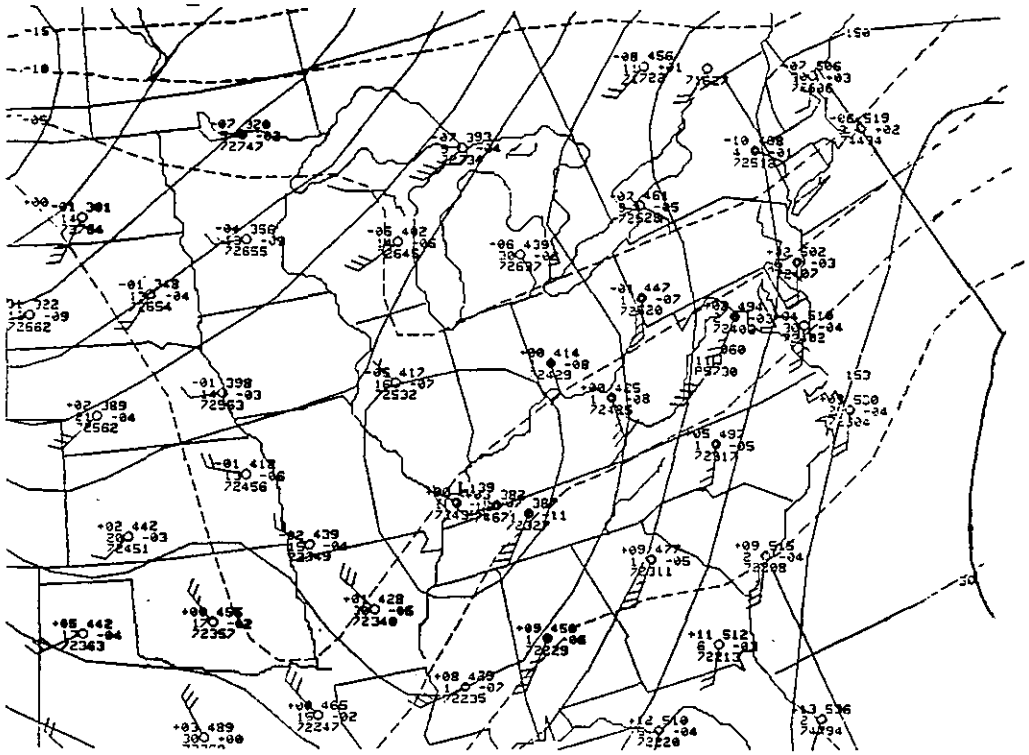

Figure 11. LFM 850-mb height (dm; solid lines) and temperature (°C; dashed lines) analyses for 1200 UTC 29 January 1990. Standard notation is used for station models; dew point depressions ≤ 5°C are shaded.

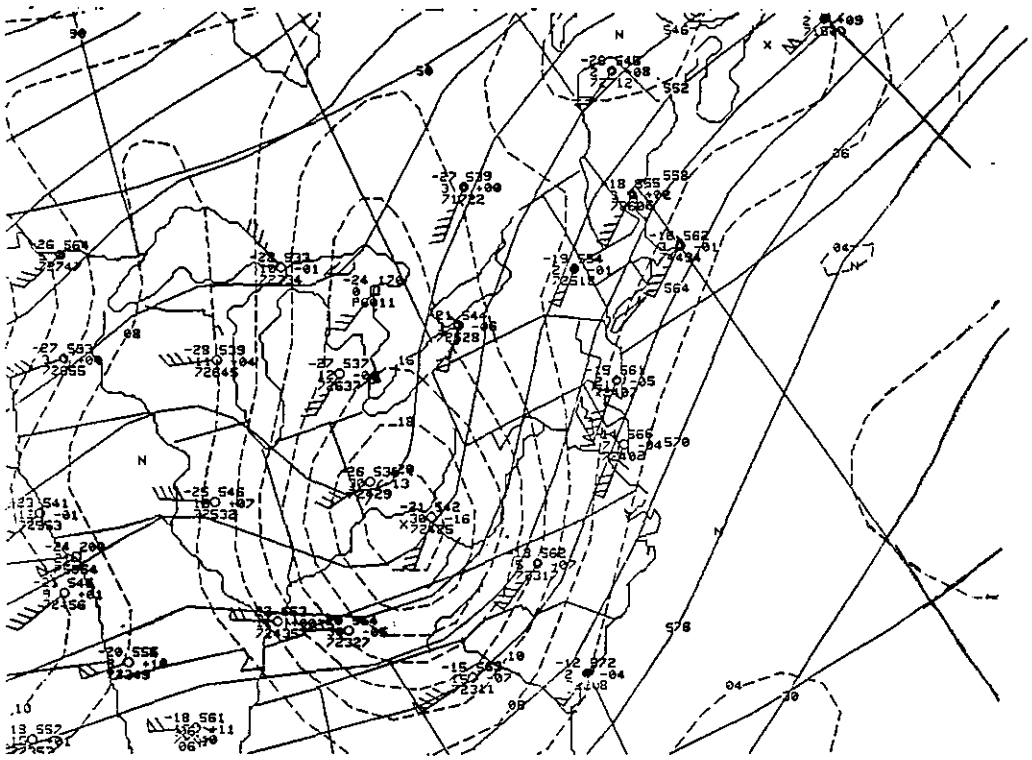

Figure 12. As in Figure 9, except for 0000 UTC 30 January 1990.

England (Figs. 12, 13, 14). At 850 mb, the 0°C isotherm made significant northward progress into southern New England, and the thermal gradient tightened along the coastal front (-9°C at Portland and +4°C at Chatham, MA [CHH]). The LFM isotherm analysis in Figure 14 does not capture this temperature gradient well. Strong southerly flow perpendicular to the tight thermal gradient coincided with the rapid spread of precipitation throughout New England during the afternoon of 29 January, and by 0000 UTC 30 January, much of southern New England had seen a changeover from snow to rain as the low levels warmed above freezing.

At 1200 UTC 30 January (Fig. 15), the 500-mb trough moved into southern New England and continued to strengthen as it developed a negative tilt. The vorticity maximum increased to 24 x 10^{-5} s^{-1} over central Massachusetts, as a 105 kt jet maximum crossed Cape Cod. Large 12-h 500-mb height falls--19 dm at Chatham; 18 dm at Albany; and 17 dm at Portland--associated with strong positive vorticity advection (PVA) were evident ahead of the trough axis. Temperatures at 850 mb (Fig. 16) had warmed to -3°C at Portland, while remaining +4°C at Chatham, with the 0°C isotherm just off the Maine and New Hampshire coasts. A closed 850-mb low was located just south of Portland with 60-kt southwest winds reported at Chatham and 40-kt east winds at Portland.

During the next 12 h, the 500-mb trough and associated vorticity maximum (not shown) moved across Nova Scotia, while a 500-mb ridge built across New England, accompanied by improving weather conditions.

2C. Precipitation

On 29 January, snow spread rapidly northward reaching southern New Hampshire by 1500 UTC (1422 UTC at Concord, NH [CON]) and northern New Hampshire and southern Maine by 1800 UTC (1720 UTC at Augusta, ME [AUG]). The snow shield spread across all of northern Maine by 0300 UTC 30 January. At times, the snow mixed with or changed to ice pellets and freezing rain over southern New Hampshire and southern Maine, especially near the coast, but generally stayed all snow over the interior. At Bangor, ME (BGR), the snow mixed with ice pellets for a period of less than two hours (from 1035 to 1225 UTC 30 January), while at Augusta, the snow mixed with ice pellets for over seven hours (from 0627 to 1404 UTC 30 January). Along the coast, at Portland, and over southern New Hampshire, the snow frequently mixed with, and occasionally changed over to, ice pellets during the early morning hours of 30 January. Some freezing rain was reported at Concord for a short time from 0745 to 0811 UTC.

The snow ended from south to north across the two state area on 30 January, between 1400-1500 UTC across Concord and Portland and finally ended at Caribou, ME (CAR), just before 0000 UTC 31 January. Total snow accumulations across New Hampshire and Maine exceeded 8 in, except along the immediate coast of New Hampshire, where amounts were generally 3-7 in. Snowfalls in excess of 18 in occurred in the higher elevations of south central New Hampshire and western Maine.

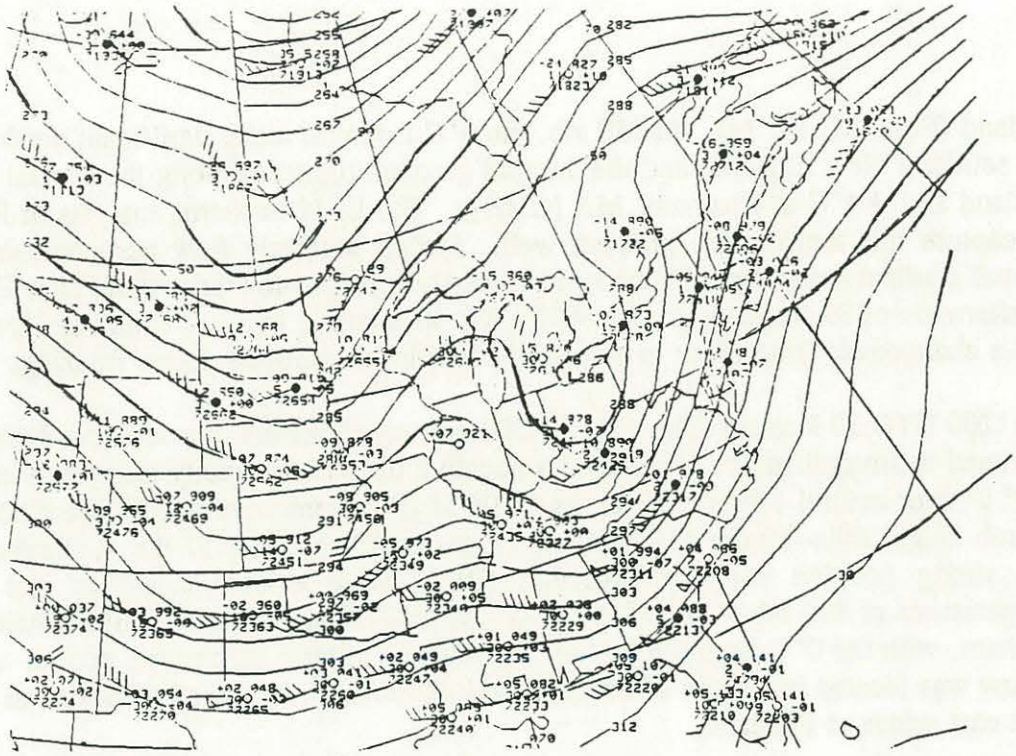

Figure 13. As in Figure 10, except for 0000 UTC 30 January 1990.

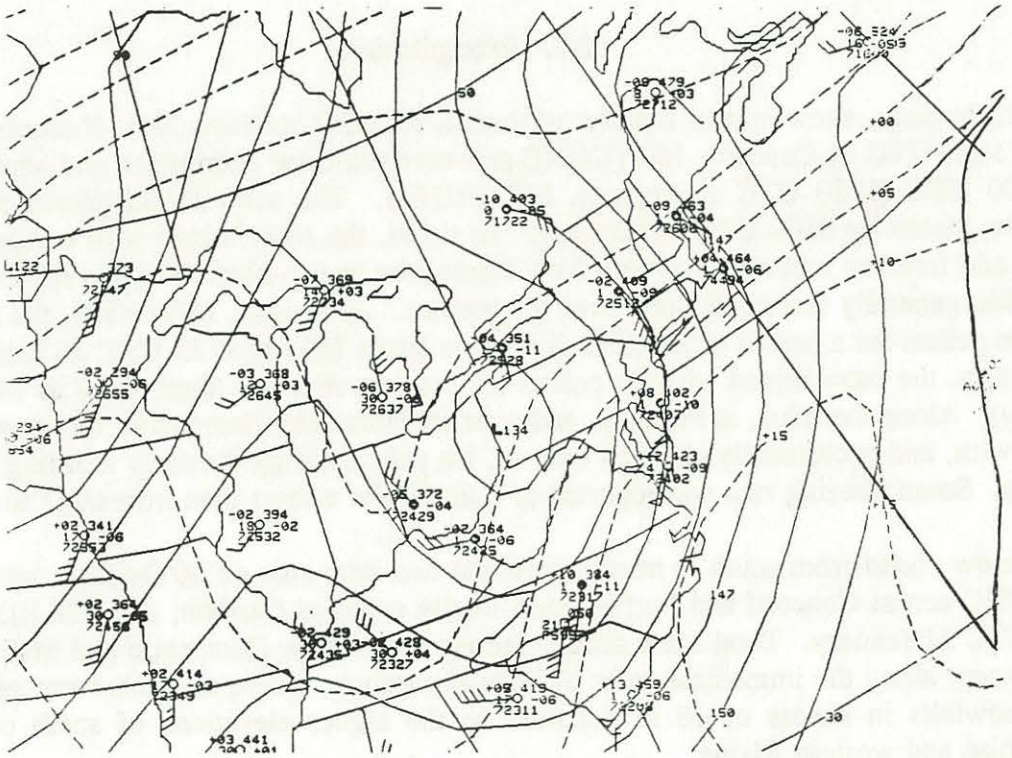

Figure 14. As in Figure 11, except for 0000 UTC 30 January 1990.

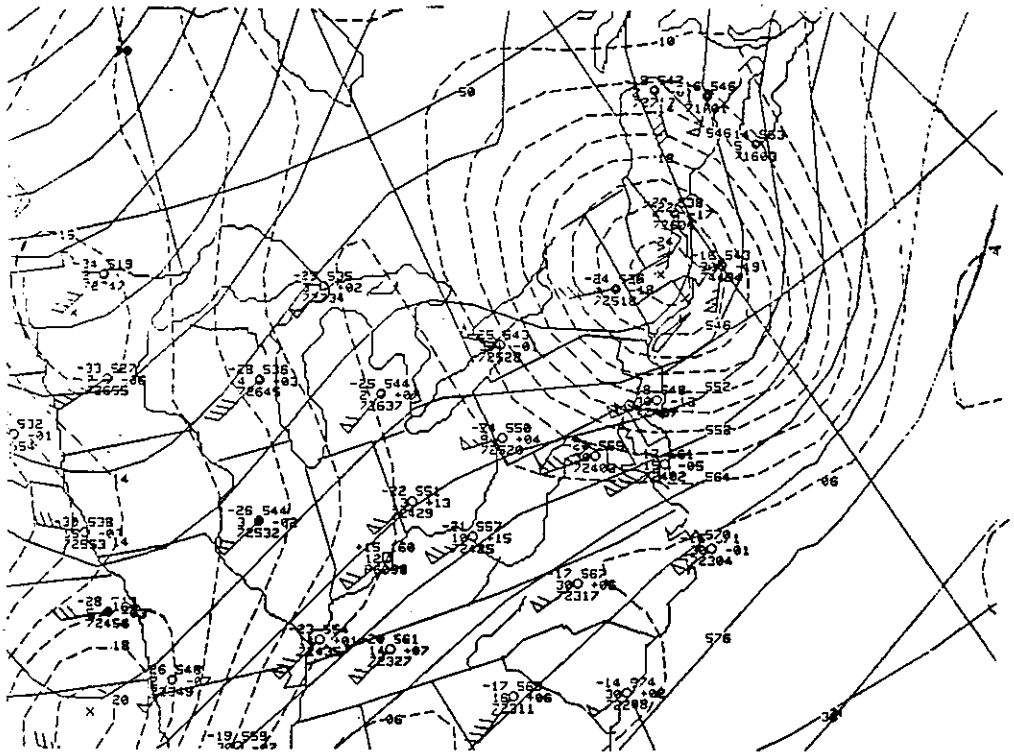

Figure 15. As in Figure 9, except for 1200 UTC 30 January 1990.

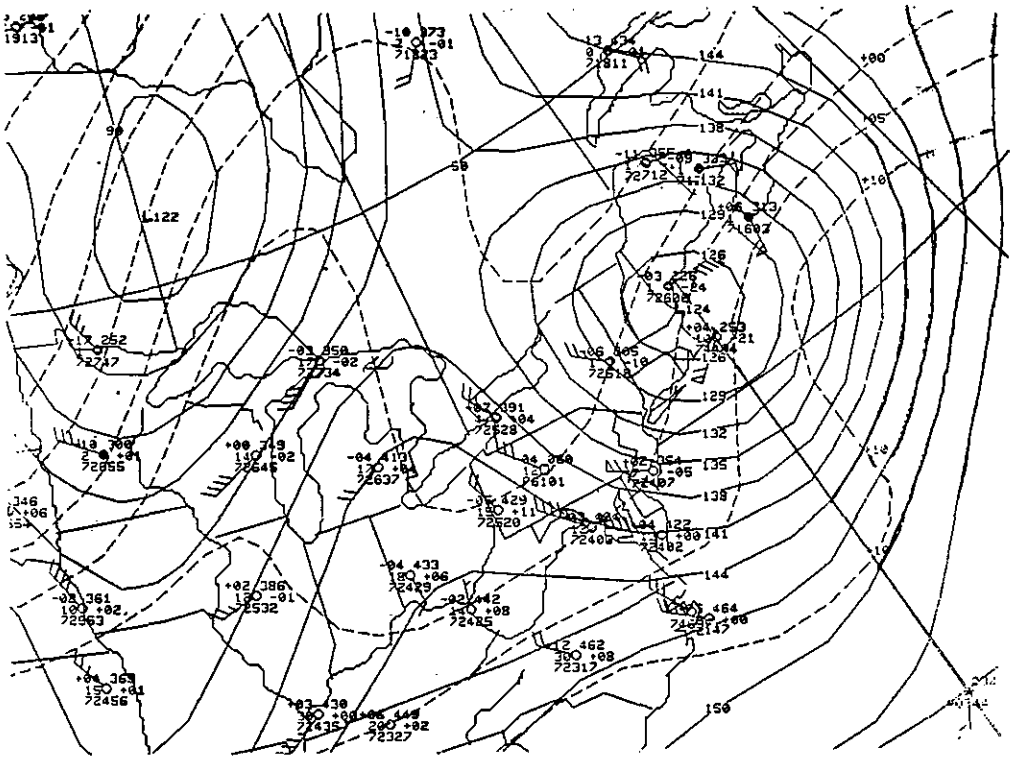

Figure 16. As in Figure 11, except for 1200 UTC 30 January 1990.

3. OTHER METEOROLOGICAL CONSIDERATIONS

A thorough analysis and understanding of synoptic-scale features at the surface and aloft are important and necessary in preparing forecasts. However, the additional effects of mesoscale features, topography, and other local conditions can also have a major impact on the forecast outcome and require a forecaster's attention.

3A. The Coastal Front

With a cold, arctic surface high positioned northeast of New England, and a surface ridge extending southward along the coast, the typical New England coastal front sets up in a corridor from Cape Cod northeast along the northern New England shoreline, often starting as an inverted trough north of a developing warm frontal wave (Bosart et al. 1972; Bosart 1975; Kocin and Uccellini 1990; McCarthy 1977; Nielsen 1989). Cold air damming is common over the northeastern United States when there is upper-level confluence over the region, resulting in low-level, northerly ageostrophic winds. However, low-level winds over the ocean are more responsive to the pressure gradient and usually maintain an easterly, or even southeasterly, component. This cyclonic turning of the low-level winds enhances the baroclinicity and low-level convergence near the coast. The coastal front forms in the baroclinic zone, between the cold arctic air over land to the north and west, and the relatively warmer air over the ocean to the south and east (see Figs. 4 and 5).

During this event, the surface low tracked along the coastal front, which remained only several miles offshore. This is a common occurrence along the New England coast, and forecasters often base their storm track and precipitation-type forecast on the expected location and movement of the coastal front. The coastal front frequently enhances precipitation amounts on the cold side of the frontal boundary (Marks and Austin 1979; Bosart 1975). For instance, in many cases where the coastal front moves onshore, the surface low hugs the coast or may even track inland, which results in low-level warming and a changeover from frozen precipitation to rain over a large area, with heavy snowfall confined to the interior locations. Conversely, heavy snowfalls occur up to the coast when the coastal front remains offshore.

The coastal front remained offshore during much of this event, oriented from northeast to southwest; although the northern end of the front shifted westward onto the eastern Maine coast as the storm center crossed Cape Cod. Later, when the storm moved into the Gulf of Maine and continued to intensify, the coastal front dissipated into the coastal circulation.

3B. Jet Streaks

The importance of jet stream dynamics in the process of cyclogenesis and its associated precipitation has been examined extensively by Uccellini and Kocin (1987) and Kocin et al. (1989). Figure 17 shows a composite of two interacting jet streaks in the Northeast and the associated low-level features, as described by Kocin et al. (1989). The transverse circulations associated with a jet streak result in rising motion in the left front (exit) and right rear (entrance)

quadrants of the jet. Upward vertical motion is enhanced when these two circulations occur in close proximity to each other. Simultaneously, subsidence in the confluent flow on the left rear quadrant of the jet helps build surface pressures north of the jet axis; in this case, across northern New England. At lower levels (850 mb), an east to southeast low-level jet (LLJ) strengthens ahead of the intensifying surface low. The LLJ works like a conveyor belt advecting and lifting relatively warm, moist air from the Atlantic Ocean into the developing storm system's three-dimensional circulation.

For this storm, an intense jet streak over southeast Canada, with winds greater than 150 kt, is shown in the 300-mb analysis at 0000 UTC 30 January (Fig. 18). Much of New England lay in the right rear quadrant, which is favorable for large scale ascent and northerly ageostrophic winds. A second weaker jet streak (80-100 kt) extended from the south central United States northeastward to the Middle Atlantic Coast. The left front quadrant covered the central Appalachians into southern New England. The coupling of these two jet streaks appeared to play a key role in the development of the system. The upper-level confluence over the Northern Appalachians into southern Canada led to the cold air damming. Explosive deepening of the surface low occurred over the Delmarva Peninsula as the left front quadrant of the southern jet streak crossed the region. The low-level jet increased to 60 kt at 850 mb (Fig. 14), advecting warm moist air into the system.

3C. Evaporational Cooling

The thermodynamic profile of the lower troposphere, below 700 mb, is critical in predicting precipitation type. Forecasters must consider the temperature and moisture profiles and look for any above freezing layers that could result in mixed precipitation or a changeover to rain. Software is available to calculate wet bulb temperatures based on sounding data and determine the potential for evaporative cooling due to precipitation falling through a dry layer. Thus, even if the low-level temperatures start out slightly above freezing, the evaporational cooling process can drop the values below freezing and result in frozen, rather than liquid, precipitation.

The vertical wind profile can be used to infer thermal advection through layers of the atmosphere. Winds veering with height are associated with warm advection, while winds backing with height indicate cold advection through the layer. A steady state can develop if warm advection is offset by evaporational cooling. However, once the sounding is saturated, the temperature of the layer will be controlled by thermal advection, with only a slight effect of moist adiabatic cooling due to upward vertical motions, and an even lesser influence of entrainment of colder air as precipitation falls through the layer.

The sounding for Portland at 1200 UTC 29 January includes the temperature, dew point, and wet bulb traces (Fig. 19), as produced by the SHARP workstation (Hart and Korotky 1991). By taking into account the effect of evaporational cooling alone, the sounding shows that the ambient temperature could cool from -6.5 to -11°C at 850 mb. In fact, 12 h later, at 0000 UTC 30 January, the Portland sounding (Fig. 20) was nearly saturated at all levels, with an 850-mb temperature of -9°C, despite indications of warm air advection at this level due to south-

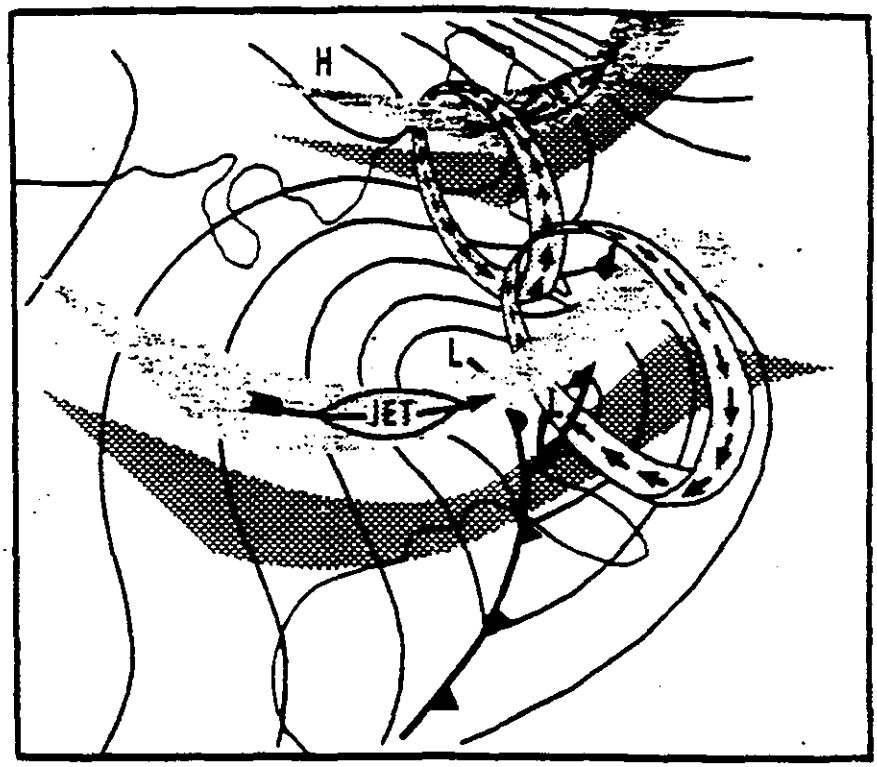

Figure 17. Three-dimensional schematic of jet-related circulation patterns during major East Coast snowstorms (from Kocin et al. 1989).

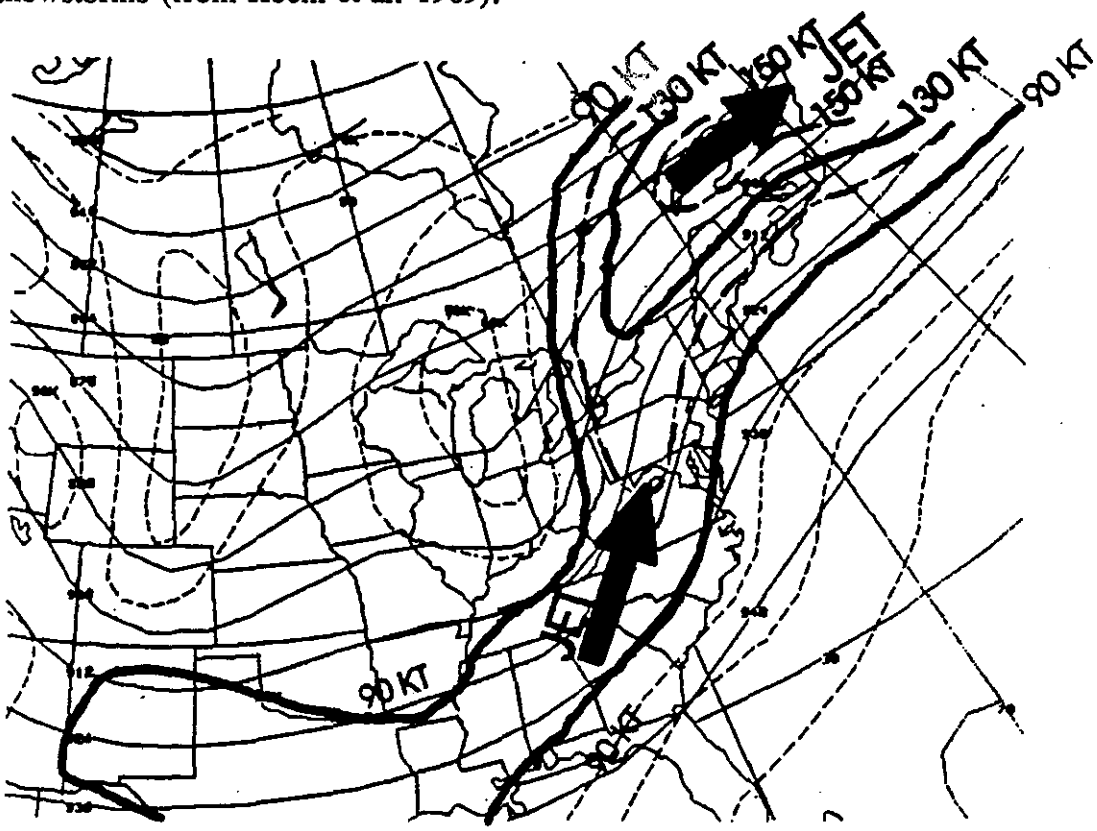

Figure 18. LFM 300-mb height (dm; solid lines) and isotach (kt; dashed lines) analyses for 0000 UTC 30 January 1990.

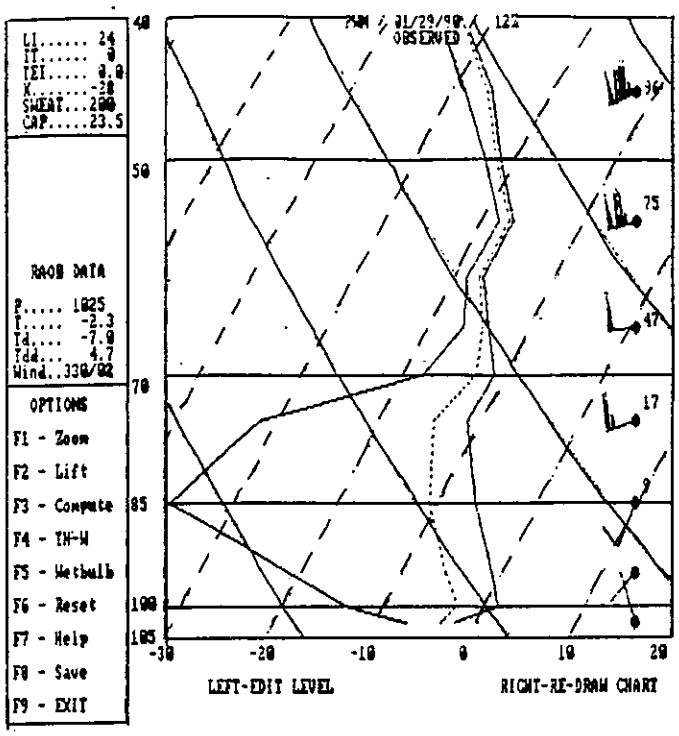

Figure 19. Skew-T/log p diagram of the Portland, ME, upper air sounding for 1200 UTC 29 January 1990 from the SHARP Workstation. Solid lines represent temperature and dew point; dashed line represents the wet-bulb trace.

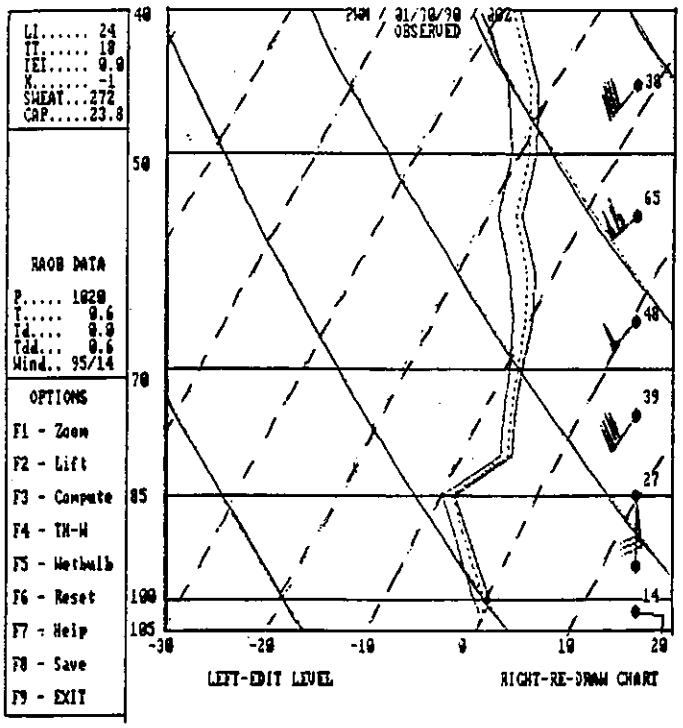

Figure 20. As in Figure 19, except for 0000 UTC 30 January 1990.

southeasterly winds and also implied from the winds veering with height. Up to this time, the warm air advection was probably offset by evaporational cooling. Since the entire sounding was below freezing, snow was falling throughout the region.

At 1200 UTC 30 January, the Portland sounding remained saturated and had warmed to -4°C at 850 mb (Fig. 21). Below 850 mb, the cold air was entrenched as the coastal front remained offshore. Northerly low-level winds persisted as cold air drained southward (east of the mountains) from the arctic high located northeast of New England. However, the sounding also revealed a layer of above freezing temperatures above the 850-mb level, where the winds shifted from north to south-southwest bringing in relatively, warm moist air. This is a typical ice pellet sounding, where the snow melts in a warm layer, but then refreezes as it falls through the deep sub-freezing layer down to the ground.

The Albany soundings at 0000 and 1200 UTC 29 January (not shown) had characteristics similar to Portland. Farther to the southeast, the Chatham soundings (also not shown) were saturated by 0000 UTC and strong warm advection produced a thick layer of above freezing temperatures that extended through the 850-mb level. A tight thermal gradient developed over southern and central New England as the Portland-Chatham 850-mb temperature difference increased from 1°C at 1200 UTC 29 January to 13°C, 12 h later.

3D. Orographically Enhanced Precipitation

Strong onshore flow supplied a continuous source of Atlantic moisture across northern New England. As depicted in the Portland sounding (Fig. 20), the depth of this strong low-level onshore flow extended to about 6000 ft AGL at 0000 UTC 30 January. Observed winds from Mount Washington, NH, (elevation 6288 ft) are used as a gage of low-level flow, with data available on a three hourly basis. In this case, winds peaked from the east and southeast in excess of 43 kt, with gusts as strong as 59 kt at 0900 UTC 30 January.

The onshore flow was perpendicular to the mountainous terrain over the interior of New England (Fig. 22), and orographic lifting served to enhance the rate of precipitation. Thus, the heaviest snowfall amounts were observed on the upslope, windward (east) side of the mountains in New Hampshire and Maine, while the minimum amounts were observed on the downslope, leeward (west) side (cf. Fig. 1).

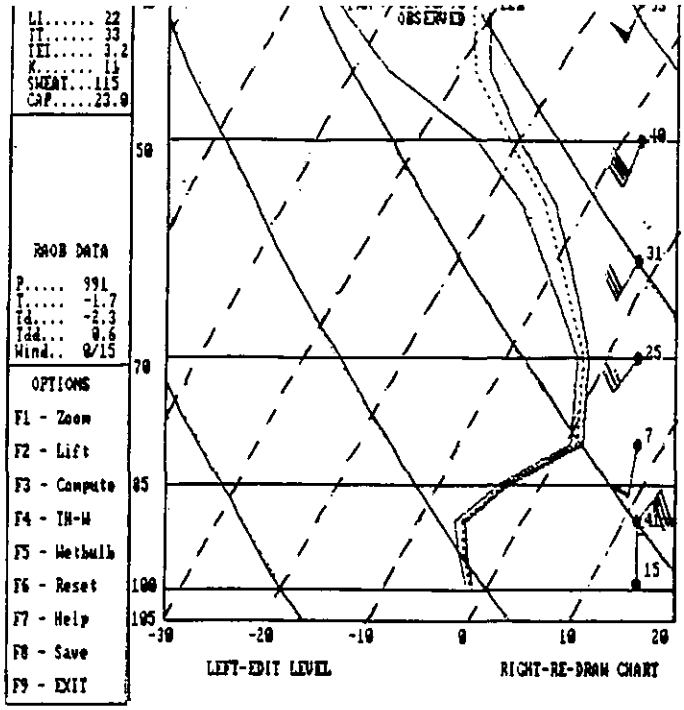

Figure 21. As in Figure 19, except for 1200 UTC 30 January 1990.

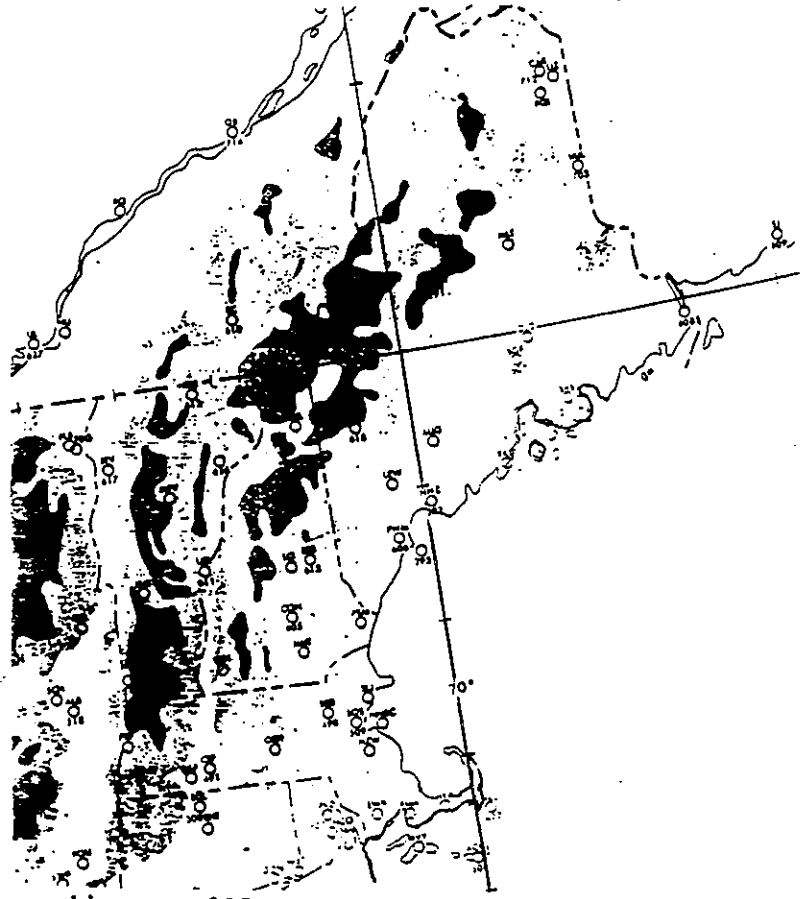

Figure 22. Topographic map of New England. Light shaded areas are elevations greater than 1000 ft MSL; dark shaded areas are elevations greater than 2000 ft MSL.

4. NATIONAL METEOROLOGICAL CENTER (NMC) MODEL PERFORMANCE

This section qualitatively compares the NMC numerical prediction model forecasts of surface and upper air features for this event. In addition, a close examination of the model quantitative precipitation forecasts (QPF) will exhibit certain strengths and weaknesses of the models for this case.

4A. Surface and Upper Air Forecasts

A comparison was made of the three dynamical computer models run from the 1200 UTC 29 January 1990 forecast cycle (Fig. 23), which was the last model guidance available to the forecasters prior to the event. Both the Nested Grid Model (NGM) and Limited-area Fine Mesh (LFM) model forecast the surface low to track too far north across the interior of southern New England. This is a documented tendency (Junker et al. 1989) of the NGM. The Aviation (AVN) model had a much better forecast, as it developed a separate low in Virginia, which then tracked across Long Island, NY, to near Boston and across the Gulf of Maine.

Although NMC has data on forecast storm tracks with 6-h resolution out to 48 h for the NGM and 72 h for the AVN, data at this resolution for these projections are not available to field offices. This can result in missing details of a storm's forecast track and evolution. For instance, in this case, the storm took a turn towards the north and hugged the eastern New England coastline between 1200 and 0000 UTC on 30-31 January. This was not evident in any of the models due to the lack of temporal resolution. Even though the AVN model did an excellent job of forecasting the low positions at 1200 UTC and 0000 UTC, a straight line interpolation between the two points was incorrect. Forecasters need to account for this shortcoming when determining model forecast tracks of surface (and upper air) features.

All of the models overforecast the central pressure of the storm as it underwent rapid intensification. However, the NGM produced the best pressure forecast. At 1200 UTC 30 January, the observed central pressure was 986 mb, while the NGM, LFM, and AVN forecasts were 992, 999, and 999 mb, respectively. Both the LFM and NGM typically underdevelop cyclones over the Atlantic, especially off the New England coast (Junker et al. 1989).

Another important consideration is the location and movement of the arctic high pressure center located to the north. Local studies have shown that the models, particularly the LFM, typically move cold highs, such as this one, east too quickly. The vertical resolution in the boundary layer, and topography in current operational NMC dynamical models, may account for why these models have difficulty with mesoscale features such as cold air damming and coastal frontogenesis (Kocin and Uccellini 1990).

The performance of the models at 500 mb was assessed based on the track of the vorticity maximum associated with the short-wave trough (Fig. 24). All three models were similar and generally handled this feature quite well, although the NGM had the best track, but was too slow at 1200 UTC 30 January.

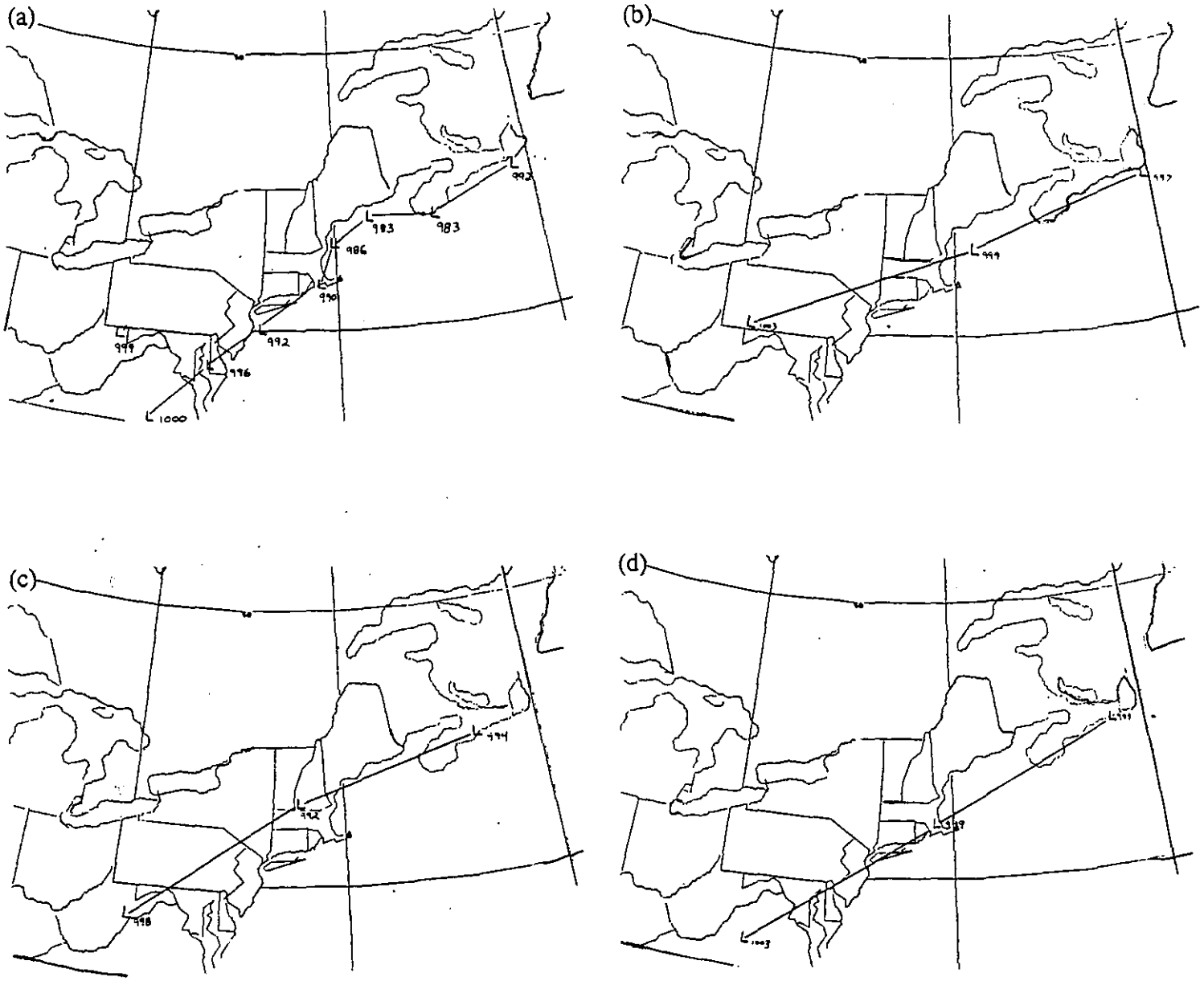

Figure 23. Track and central pressure of surface low as: (a) observed (LFM analysis), where L depicts the low every 3 h from 0000 through 1800 UTC 30 January 1990 and at 0000 UTC 31 January 1990 and L' represents the original low at 0000 UTC 30 January 1990, (b) LFM forecast, (c) NGM forecast, and (d) AVN forecast. The forecasts are 12-, 24-, and 36-h projections from 1200 UTC 29 January 1990.

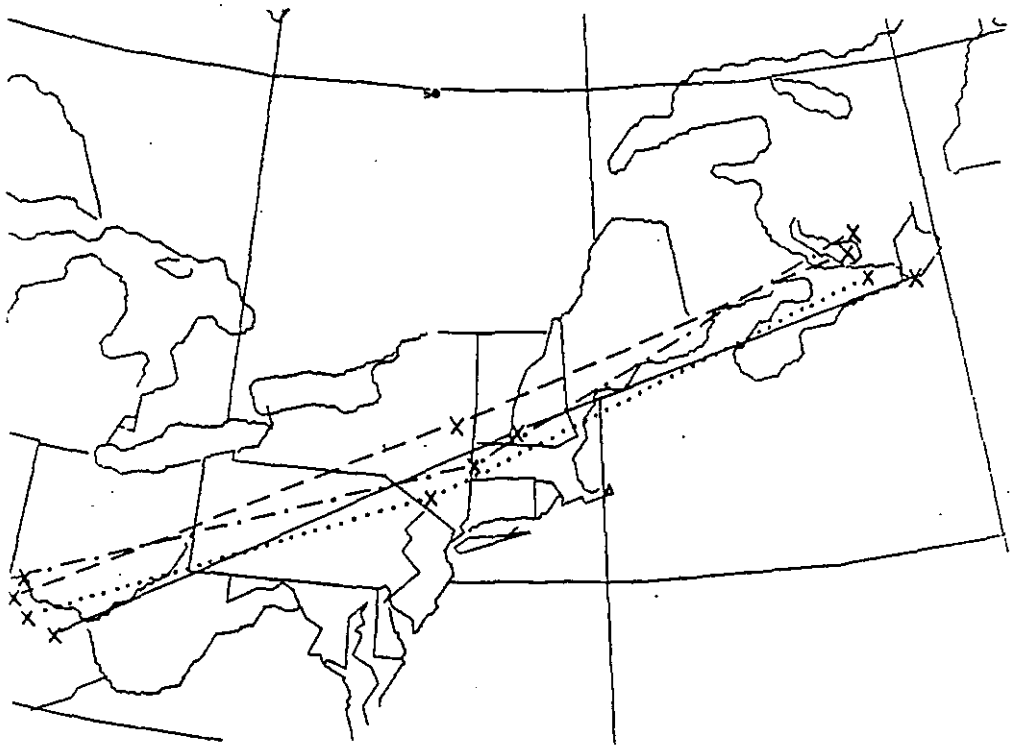

Figure 24. Track of the 500-mb vorticity maximum. Representations are: solid line for the observed (LFM analyses) track, dashed line for the LFM forecast, dotted line for the NGM forecast, and dash-dot-dash line for the AVN forecast. The observations are every 12 h beginning at 0000 UTC 30 January 1990. Forecast times are the same as in Figure 23.

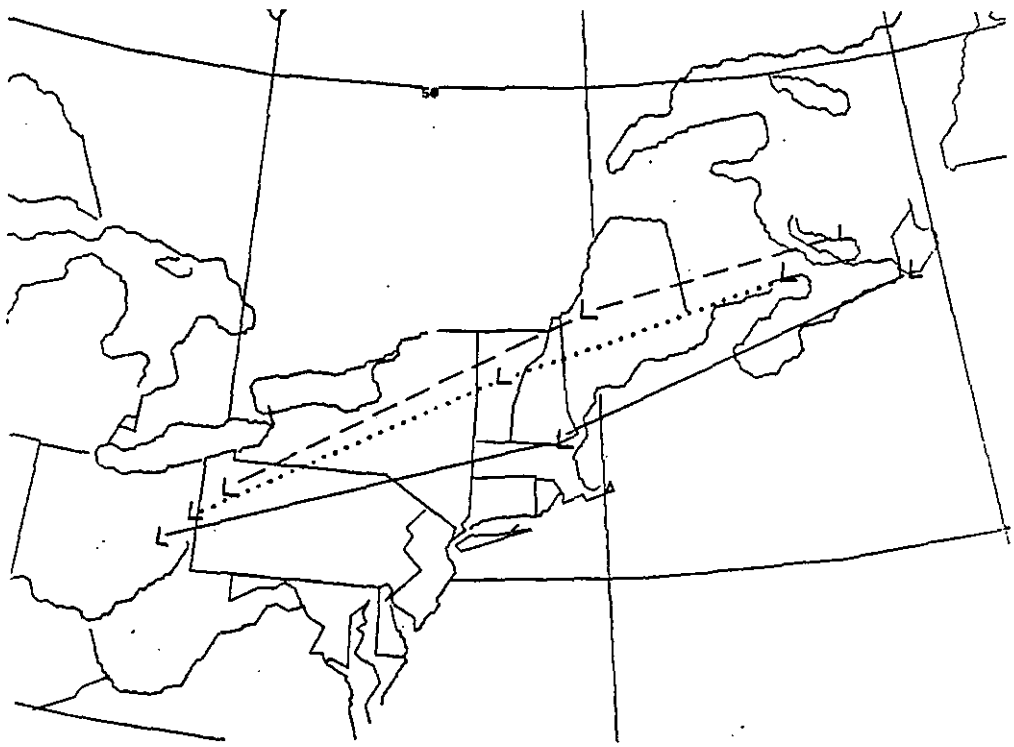

Figure 25. As in Figure 24, except for the 850-mb low center (not available from the AVN).

The NGM and LFM models forecast the track of the 850-mb low too far inland (Fig. 25). (Note, the AVN 850-mb prognostic charts were not available.) As a result, both models produced excessive low-level warming over southern New Hampshire and southern Maine. The observed track of the 850-mb low along the southern New Hampshire border and into the Gulf of Maine south of Portland cut off the low-level warming before a changeover from snow to rain could occur.

4B. Quantitative Precipitation Forecasts (QPF)

The LFM routinely generates too much precipitation by a factor of two in moderate-to-intense mid-latitude cyclones (Carr 1988). Therefore, forecasters at the Weather Service Forecast Office (WSFO) in Portland usually consider an adjusted LFM QPF by cutting the amount in half (Adjusted QPF = LFM QPF ÷ 2).

An analyzed plot of the adjusted LFM 48-h storm total precipitation output from the 0000 UTC 29 January detailed FOUS60 bulletin (Fig. 26a) shows an axis of maximum precipitation (> 0.75 in) across the northern half of New England. The NGM 48-h storm total QPF from the FOUE60 bulletin (Fig. 26b) shows the axis of maximum precipitation farther south across southern portions of New Hampshire and Maine, with amounts close to 1 in. The 1200 UTC 29 January LFM increased its adjusted maximum QPF up to around an inch, with the axis along the coast of Maine (Fig. 26c). The 1200 UTC NGM run increased the maximum QPF to about 1.50 in over southwest Maine (Fig. 26d). All of these model forecasts were too low with actual amounts in excess of 1 in throughout New England with 1.5-2.0 in over the interior upslope locations (Fig. 27). Also, both models forecast the maximum precipitation axis too far south, despite forecasting the track of the surface and 850-mb lows too far north. Orographic influence would, in part, explain this error.

Using commonly accepted snow-to-liquid water ratios for the Northeast, and assuming an all snow event, snowfall forecasts based solely on QPF can be quickly prepared. Output from the 1200 UTC 29 January model runs, using a standard 10-to-1 ratio for wet snow along coastal areas would produce a forecast around 15 in of snow based on the NGM QPF and just under 10 in based on the adjusted LFM QPF. Over the interior, the snow is usually drier and the ratio can be greater than 10-to-1. For this system, all models pointed to the likelihood of a heavy snowfall in those areas that did not change to rain.

The LFM quite often forecasts one inch amounts that are rarely observed in Maine and New Hampshire (Capriola 1990). Using this guidance alone can result in a high false alarm ratio. Conversely, the NGM model rarely forecasts QPF in excess of one inch over a 12- to 18-h period, the time span when the majority of the precipitation would normally fall during a heavy snow event in the Northeast. In the two years prior to this storm, only two other events of this magnitude were predicted by the NGM for Maine and New Hampshire. The NGM usually is a conservative forecaster of QPF and may underforecast heavy precipitation events in northern New England during the winter season (Capriola 1990). Therefore, large QPF generated by the NGM should cause particular concern, especially if corroborated by the adjusted LFM output.

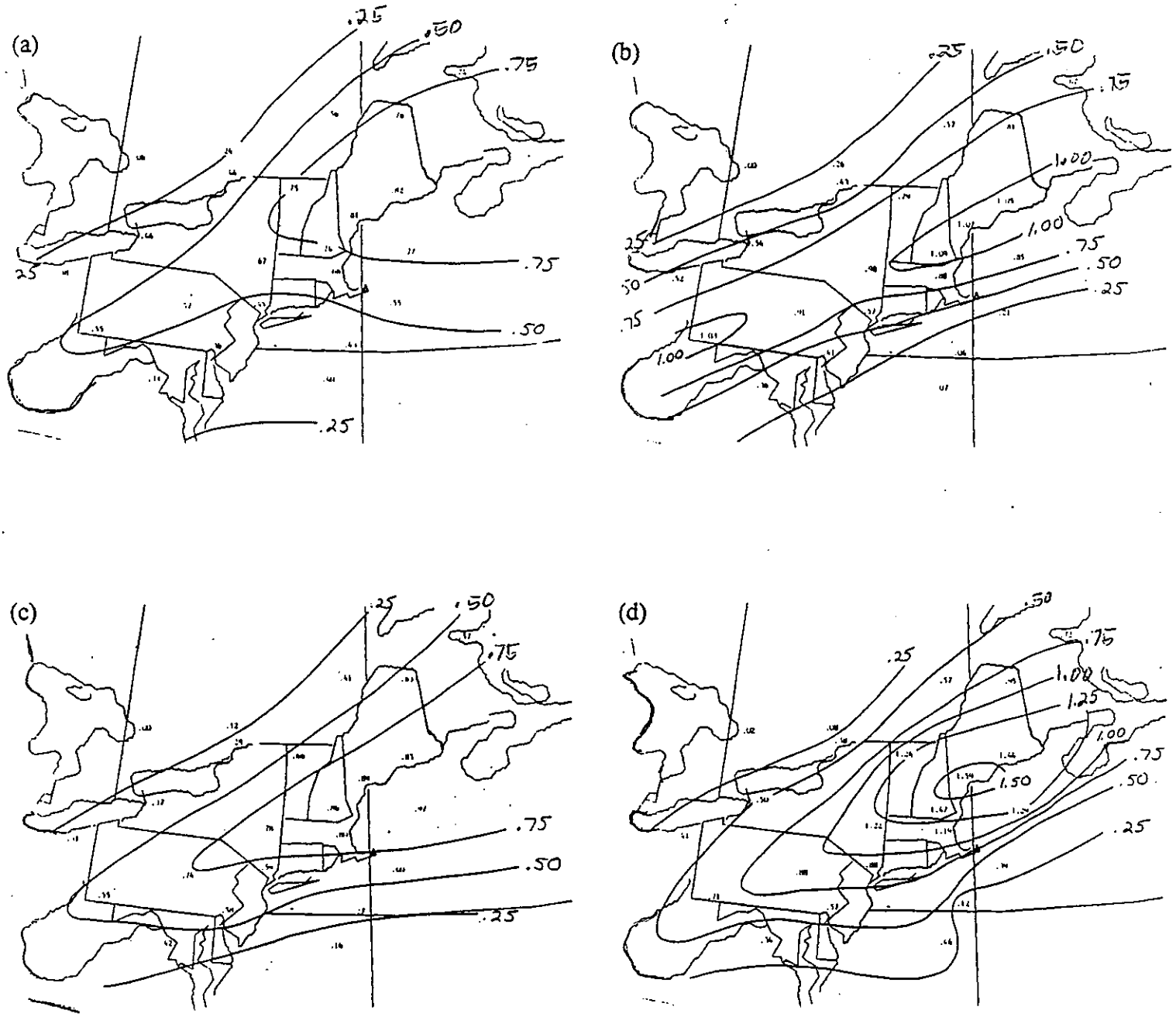

Figure 26. Storm-total (48-h) QPF from the 0000 UTC 29 January 1990 run of the (a) LFM (adjusted) and (b) NGM, and the 1200 UTC 29 January 1990 run of the (c) LFM (adjusted) and (d) NGM. Contours are every .25 in.

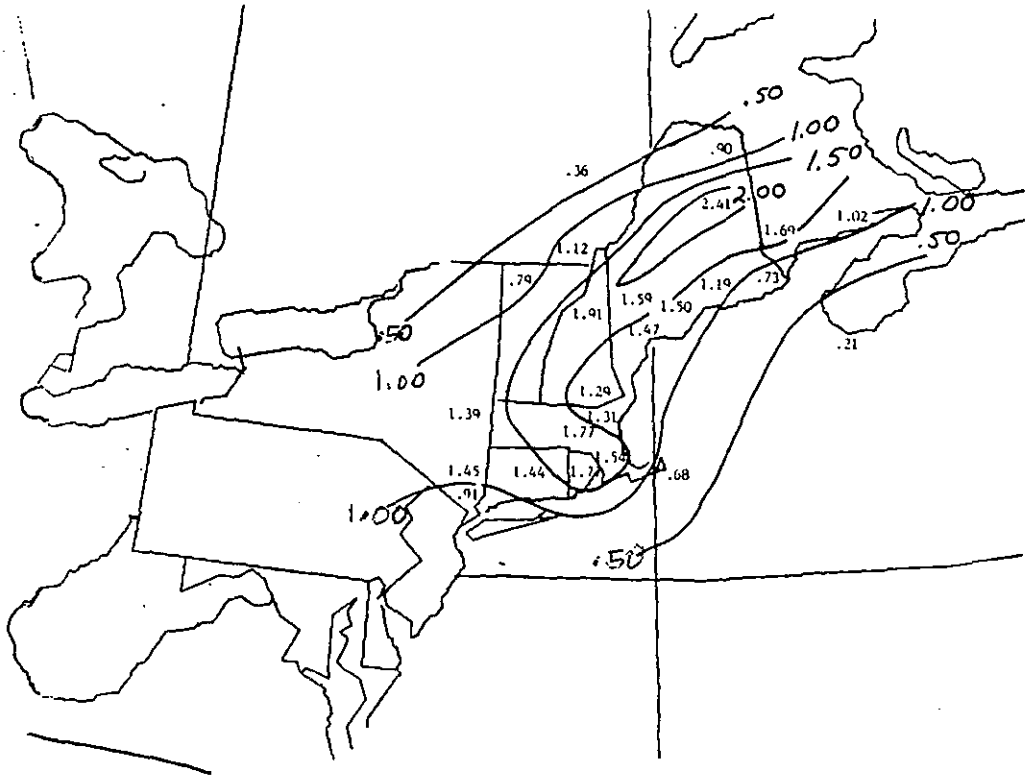

Figure 27. Storm-total (48-h) observed liquid equivalent precipitation ending at 1200 UTC 31 January 1990. Contours are every .50 in.

Table 1. Alphanumeric output of 48-h precipitation from the 0000 and 1200 UTC 29 January 1990 model runs of the LFM and NGM for Portland, Caribou, Bangor, and Concord.

	PWM	CAR	BGR	CON
0000 UTC 29 January 1990				
NGM	1.07	0.81	1.05	1.09
LFM	1.61	1.52	1.64	1.48
Adjusted LFM	0.81	0.76	0.82	0.74
1200 UTC 29 January 1990				
NGM	1.59	0.95	1.44	1.47
LFM	1.78	1.26	1.66	1.71
Adjusted LFM	0.89	0.63	0.83	0.86
STORM TOTAL OBSERVED PRECIPITATION	1.47	0.90	1.19	1.29

A comparison of both the LFM and NGM precipitation forecasts at specific locations (Table 1) shows that the NGM outperformed the LFM at Portland, Caribou, Bangor, and Concord. Generally, the adjusted LFM QPF was a better forecast than the actual LFM output; although, the adjusted LFM output (and the NGM) consistently underforecast the amounts. As noted by Junker et al. (1989), the NGM tends to underforecast heavy precipitation during the winter. The NGM's documented low bias for the first 6-h period (Jensenius 1989) may have affected the 1200 UTC 29 January run. Nevertheless, the NGM model run from this time was the most accurate forecast of those available.

5. APPLICATIONS OF NMC GUIDANCE

Several applications of NMC guidance are used to prepare winter storm warnings and forecasts. These empirical methods include local studies on precipitation types, a "Bomb" or explosive cyclogenesis checklist, and the use of the "magic chart." This section looks at the use of these forecast aids in this case.

5A. Precipitation Type

At WSFO Portland, a locally-derived procedure is used to predict precipitation type (i.e., liquid, freezing, or solid), contingent on the occurrence of precipitation (Ronco 1988). This two part prediction uses the NGM model FOUS low-level temperature forecasts and the Model Output Statistics (MOS) probability of frozen precipitation (POF) from the LFM for Portland, Bangor, Caribou, and Concord. Three categories of precipitation type are defined. The liquid precipitation category includes rain and freezing rain, the solid precipitation category includes snow and ice pellets, and the mixed category is any combination of precipitation types from the first two categories. Table 2 shows this output based on the 1200 UTC 29 January models.

The output is for 6-h periods (coincident with NGM FOUS and LFM MOS output), beginning with a 6-h forecast from model initialization time. Part I shows the relationship of low-level temperature predictions (T1, T3, and T5) from the NGM (Part I output uses the same format for temperatures as the NGM FOUS) and the associated probability of precipitation type based on statistical studies for each site. Part II integrates the LFM MOS POF guidance with the NGM low-level temperature forecasts and produces a combined probability of precipitation type.

Critical values used by forecasters are empirically derived. Generally, probability forecast thresholds of 50% are used to forecast rain or snow. A forecast of 10% or greater for the mixed category suggests the potential for freezing rain and/or ice pellets.

For Caribou, both parts of the procedure correctly predicted an all-snow event. For Bangor, the Part I prediction was for a brief changeover of snow to rain, before a changeover back to snow would occur. The Part II prediction indicated that the precipitation would remain all snow, with never less than a 63% chance of snow. In actuality, the precipitation was snow, with only a brief period of ice pellets. For Portland, the NGM-based guidance supported snow, followed by a prolonged period of rain that would change back and end as snow. The combined output predicted a similar situation, but indicated a shorter period of liquid precipitation. The observed precipitation was mainly snow, with a considerable period of sleet, or a mixture of the two. For Concord, the predictions and observations were almost identical to Portland, except that a brief period of freezing rain occurred.

Overall, Part II of the modified guidance was colder than Part I; that is, it had higher probabilities of frozen versus liquid precipitation, and was better in this case. The reason for this was due in part to the LFM forecast of a colder storm track along the coast, as compared to the NGM track of the low inland. However, both model forecasts were still too warm,

Table 2. Precipitation-type forecasts (Ronco 1988) from the 1200 UTC 29 January 1990 model runs. NGM temperatures are in °C; POF is in percent; and rain, snow, and mix are probabilities.

T1T3T5 FROM NGM 12Z JAN 29 90

PWM

HR	T1	T3	T5	RAIN	SNOW	MIX
6	0	95	92	.033	.926	.041
12	0	96	97	.168	.736	.096
18	2	0	1	.871	.072	.049
24	3	3	2	.968	.032	.000
30	2	97	99	.650	.200	.150
36	0	97	2	.409	.409	.182
42	97	98	97	.168	.736	.096
48	0	0	95	.113	.825	.062

CAR

HR	T1	T3	T5	RAIN	SNOW	MIX
6	96	93	88	.000	1.000	.000
12	98	95	88	.000	1.000	.000
18	95	94	91	.000	1.000	.000
24	94	90	96	.019	.954	.027
30	94	89	91	.000	1.000	.000
36	91	88	88	.000	1.000	.000
42	87	90	94	.014	.967	.019
48	87	92	93	.012	.971	.017

BGR

HR	T1	T3	T5	RAIN	SNOW	MIX
6	0	96	90	.000	1.000	.000
12	99	94	92	.033	.926	.041
18	0	95	99	.258	.638	.104
24	0	96	0	.317	.578	.105
30	1	97	97	.529	.353	.118
36	98	95	99	.258	.638	.104
42	94	94	99	.043	.922	.035
48	94	98	95	.113	.825	.062

CON

HR	T1	T3	T5	RAIN	SNOW	MIX
6	0	95	94	.099	.844	.057
12	0	97	97	.168	.736	.096
18	3	3	2	.968	.032	.000
24	4	3	1	.871	.072	.049
30	1	96	99	.625	.214	.161
36	99	98	1	.361	.532	.107
42	0	99	97	.168	.736	.096
48	0	0	95	.113	.825	.062

****

PWM 29/12Z

HR	POF	RAIN	SNOW	MIX
6	98	.007	.986	.007
12	82	.123	.827	.050
18	32	.801	.149	.050
24	24	.844	.119	.037
30	86	.222	.771	.007
36	67	.158	.782	.060
42	66	.158	.782	.060
48	69	.158	.782	.060

CAR 29/12Z

HR	POF	RAIN	SNOW	MIX
6	99	.000	.999	.001
12	99	.007	.986	.007
18	99	.000	.999	.001
24	98	.000	.999	.001
30	98	.000	.999	.001
36	98	.000	.999	.001
42	97	.000	.999	.001
48	97	.000	.999	.001

BGR 29/12Z

HR	POF	RAIN	SNOW	MIX
6	99	.007	.986	.007
12	97	.007	.986	.007
18	77	.123	.827	.050
24	57	.171	.754	.075
30	89	.295	.636	.069
36	90	.083	.877	.040
42	86	.014	.983	.003
48	83	.123	.827	.050

CON 29/12Z

HR	POF	RAIN	SNOW	MIX
6	97	.007	.986	.007
12	80	.123	.827	.050
18	50	.718	.201	.081
24	51	.718	.201	.081
30	90	.295	.636	.069
36	81	.123	.827	.050
42	70	.158	.782	.060
48	72	.158	.782	.060

especially in the region of low-level, cold-air damming over the interior. This error was critical since NGM temperature predictions are for low levels (assuming the surface is at 1000 mb: T1 extends from 1000-965 mb, T3 from 927-872 mb, and T5 from 816-756 mb). The warm error was in part due to the incorrect track of the model cyclone. Forecasters should adjust the low-level temperature forecasts, or select a more representative station, if they think the model storm track will be wrong.

5B. The Meteorological "Bomb" Checklist

An important concern, especially for marine forecasters, is the "Bomb," an explosively deepening low pressure system moving off the East Coast and out over the open Atlantic Ocean (Sanders and Gyakum 1980). The meteorological bomb has been defined as a low pressure system, whose central pressure drops over a 24-h period by an amount equal to, or greater than, 24 mb multiplied by the ratio of the sine of the latitude divided by the sine of 60°N (Sanders and Auciello 1989). This translates to a pressure fall of at least 20 mb per 24 h for a low crossing the coast at 45°N.

The storm's central pressure was 1009 mb at 1800 UTC 29 January and dropped 26 mb to 983 mb by 1800 UTC 30 January; thus, it met the criteria of a "bomb." As a result, storm force winds (≥ 48 kt) developed over the coastal waters of Maine and New Hampshire (Table 3).

To aid forecasters, a checklist was developed using NMC model guidance (both LFM and NGM) to determine the likelihood of a bomb development (Auciello 1989). The checklist was developed as an objective aid to forecast bombs out to 36 h within an area bounded by 38°N to 45°N latitude and 55°W to 75°W longitude. The bomb checklist contains six yes/no questions (Fig. 28) that determine the amount of upper-level dynamical forcing. The checklist requires an answer of yes on four (or more) of the six questions to determine if explosive cyclogenesis is likely to occur based on model predictions.

For the 1200 UTC 29 January 1990 run, each model scored positively on five items. Even though both models underforecast the strength of the surface low as it crossed the coast, the other five upper-level features were in place, and forecasters could anticipate a deeper surface low than was forecast by the models.

The next step after the forecaster has determined that a bomb would occur is to forecast at what time the intensifying storm system would begin to produce storm force winds. This time is referred to as "time zero" in the checklist and is the midpoint of the 24-h period when the storm deepens the most. This occurs, on average, when the overtaking 500-mb vorticity maximum is 300 mi west of the surface low. In this case, it was determined from the 1200 UTC 29 January model runs that storm force winds could be expected along the New England Coast within 12 h (around 0000 UTC 30 January).

Actually, the surface low began deepening around 1800 UTC 29 January and reached its maximum strength around 1800 UTC 30 January. Thus, the midpoint of the rapid-deepening phase of the storm occurred around 0600 UTC 30 January. Observations from buoys showed

Table 3. Hourly wind observations from buoys off the New England coast on 29-30 January 1990. Buoy identifiers are as in Figure 8; time is in UTC. Asterisks after the observation indicate that the data failed quality-control checks and were not transmitted in real time.

TIME (UTC)	44007 PWM LNB	MDRM1	MISM1	44005	IOSN3	44008	BUZM3	44013 BOS LNB
29 January								
1000	3504	3306G08	3204G06	0208G10	2904G06	0712G14	0208G10	2804
1100	0104	3406	3406	0508G10	2702G04	0714G17	0114	0000G02
1200	1004G06	3204G06	3508GMM	0908G10	0000	0716G19	0214G16	0000
1300	0908G10	3406	3608GMM	1010G14	0000G02	0917G19	0416G17	3102G04
1400	1010	0106G08	0406G08	1112G14	0000	1019G23	0319G21	0000G04
1500				1416G17				
1600	1614G19	1508G10	1308		2404	1019G23	0417G19	1708G10
1700	2116G19	1512G14	1506G08		0000	1121G25	0614	1106G08
1800	2106G08	1612G16	1617	1314G17	0304G06	1223G29	0923G25	1014G16
1900	0000	1514	1517G19	1216G19	0512	1123G29	0925G27	1017G21
2000		1516G17	1416	1221G25	1019G21	1127G33	0927G29	1119G23
2100	1319G23	1317	1319G21	1119G25	0921G25	1131G39	0825G27	1119G23
2200	1321G25	1319G21	1221G23	1121G27	0923G27	1129G35	0821G23	1121G27
2300	1123G27	1221G25	1025G27	1023G29	1033G37	1131G37	0821G25	1025G33
30 January								
0000	1225G33	1023G25	1129G33	1025G31	0925G29	1127G35	0823	0921G27
0100		1131G37	1035G39	1027G35	0825G27	1129G33	0819G21	0925G31
0200	1125G33	1131G39	1037G43	1031G35	0927G31		0314G16	
0300	1027G35	1031G41	0937G41	1029G37	0727G29	1127G33	0519G21	0823G29
0400	1027G33	0933G41	0941G45	1031G37	0629G35	1223G29	0317G19	0627G33
0500	1027G33	0941G50	0939G48	1029G39	0635G39	1717G21	0319G21	0527G33
0600	1033G43	0939G45	0943G50	0929G35	0637G41	1921G23	0119G21	0527G37

Table 3. Continued.

TIME (UTC)	44007 PWM LNB	MDRM1	MISM1	44005	IOSN3	44008	BUZM3	44013 BOS LNB
0700	0833G41	0937G47	0848G54	0931G39	0539G43	1921G23	0319	0527G33
0800	0833G45	0943G48	0837G43	1027G33	0541G47	2125G31	0314G16	0427G35
0900	0735G45	0945G52	0850G58	0919G23	0335G43	1823G27	3610G12	
1000	0635G43	0941G48	0848G56	1406G10	0239G48	2125G29	2310G14	0225G33
1100	0331G37	0950G60	0847G56	1816G19	0139G47	2433G39	2333G37	0225G33
1200	0231G37	0937G43	0845G52	2027G37	3331G37	2431G41	2725G29	3431G39
1300	3433G39	0939G47	0739G43	2129G37	3131G37	2435G45	2727G29	3031G39
1400	3337G47	1231G37	1307GMM*	2233G43	3037G41		2923G25	2831G39
1500	3235G45	1714G16	3348G56	2835G45	3121G23	2637G45	2821G23	2925G31
1600	3331G39	0000G02	3341G50	2937G47	2917G19	2633G41	2825G29	2725G31
1700	3327G33	3445G50*	3337G43	3035G45	3031G35	2729G33	2717G19	2825G35
1800	3217G25	3437G45	3237G41	2933G43	3023G29		2819G21	2927G35
1900	3217G23	3431G39	3231G37	3031G37	3027G29	2725G29	3021	2923G29
2000	2912G16	3335G41	3227G29	3127G33	3017G19	2819G25	3116	2921G27
2100	2917G21	3327G31	3121G25		2923G25	2817G21	3012GMM	2919G25
2200	3217G21	3429G31	3125G27	3121G27	3023G27	2616G19		3117G19
2300	3414G17	3425G29	3319G21	3219G27	3117G19	2617G21	2619G21	2816G17

G.....Peak gust

MM.....Peak gust missing

EXPLOSIVE CYCLOGENESIS CHECKLIST

VALID NORTH OF 40 DEGREES NORTH LATITUDE AND WEST OF 60 DEGREES WEST LONGITUDE

DATE: ___1-29-90_____ FORECAST BASE: 00Z ____ 12Z _X__

1. Does a 500mb absolute vorticity max of 15 (17-NGM) or greater exist as an initial condition for an area bounded by: 30 to 50 degrees north latitude and 85 to 110 degrees west longitude?

   LFM: YES_X_ NO____ NGM: YES_X_ NO____

2. Does this 500mb vorticity max maintain its initial intensity or strengthen on successive 12, 24, 36, 48 hour charts?

   LFM: YES_X_ NO____ NGM: YES_X_ NO____

3. Is this 500mb vorticity max forecast to move an average of 30 knots or greater through 48 hours?

   LFM: YES_X_ NO____ NGM: YES_X_ NO____

4. Does the initial 500mb vorticity max cross the coast between 32 and 45 degrees north latitude?

   LFM: YES_X_ NO____ NGM: YES_X_ NO____

5. Does a jet streak of 120 knots (110 knots-NGM) or greater exist at 250 or 300mb in a position just south of the initial 500mb vorticity max?

   LFM: YES_X_ NO____ NGM: YES_X_ NO____

6. Does the model develop a surface low of 995mb (990mb-NGM) or deeper over an area bounded by 38 to 45 degrees north latitude and 55 to 75 degrees west longitude?

   LFM: YES____ NO_X_ (997 MB) NGM: YES____ NO_X_ (992 MB)

If four or more of the above conditions are met, the situation should be closely monitored for the possibility of explosive cyclogenesis.

Assuming a perfect prognosis of 500mb vorticity by the model:

1. Time zero (the midpoint of the 24 hour period of greatest deepening) will occur when the overtaking 500mb vorticity max is 300 miles west of the surface low.

2. Storm force winds will begin close to time zero. The strongest winds will occur in the west quadrant of the system.

Figure 28. Explosive cyclogenesis ("Bomb") checklist prepared using 1200 UTC 29 January 1990 model output.

storm force winds began by 0500 UTC 30 January, in fairly good agreement with the observed deepening of the storm system. Observed storm force winds persisted through 1700 UTC, a period of 13 h (Table 3).

The model-based checklist predicted storm force winds as much as 6 h too soon, but this cannot be considered a bad forecast for two reasons. First, it highlighted the need for a storm warning, even if it led to issuing a premature warning. The extra lead time would alert the marine community. Secondly, the winds were increasing rapidly during this time period, and due to the sparse data, storm force winds may have occurred a few hours earlier than the limited network of buoys have indicated (Table 3). In fact, the coastal winds increased from less than small craft advisory strength (< 25 kt) to storm force in just eight hours (from 2100 UTC 29 January to 0500 UTC 30 January).

Time series plots of buoy data are updated frequently at WSFO Portland, and in this case clearly identified the track of the low as it moved north-northeast, hugging the New England coastline. Occasionally during this storm, buoy data were not available. There were two key instances (followed by an * in Table 3) when data were not transmitted on a real time basis. It was obtained, after the fact, upon request from the National Data Buoy Center (NDBC) in Biloxi, MS. These observations were critical as winds were changing abruptly in both speed and direction with the passage of the surface low almost directly over buoys MISM1 and MDRM1.

The NDBC checks all buoy data transmitted into the National Weather Service (NWS) Automation of Field Operations and Services (AFOS) computer network. At the time of this event there were certain time variability checks for wind speeds ($\geq$ 30 kt h^{-1}), and when exceeded, the buoy information is rejected by NMC software (Fred Abel, NDBC, personal communication), as in this event. These critical buoys had to report missing values due to the quality control conditions set by NMC. This was only the second known case from 1982 to 1990 that good data reports were deliberately thrown out.

Limits on wind speed changes for tropical storms have been routinely removed since extraordinary drops and increases in wind speeds can occur with the passage of the hurricane's eye. Since this winter event, the limits on Coastal Marine Automated Network (C-MAN) and buoy data for extratropical systems have been modified by NDBC (Dave Gilhousen, personal communication). If certain criteria of pressure changes occur in an extratropical storm with central pressures below 995 mb, then wind speeds that might have failed the original quality control procedures are re-accepted (Gilhousen 1991).

5C. The "Magic Chart"

Another guidance tool available to forecasters for winter storms is the "magic chart," described by Chaston (1989). This method uses the trajectory model (LFM-derived at the time of this event, now uses NGM) 700-mb net vertical displacement (NVD) for the 12- to 24-h period overlaid on the 12-h NGM 850-mb temperature forecast to determine areas of expected heavy

snowfall during the 12-24 h forecast period. As a rough estimate, +20 mb of NVD in the 850-mb temperature range of -3 to -5°C is equivalent to an expected snowfall of 2 in (40 mb NVD = 4 in, etc.). This technique only works for mature or developing synoptic-scale systems with adequate moisture.

This chart can be made quickly by overlaying AFOS graphics 7WG (NVD) and 82T (Fig. 29), and is valid for the 12-h period that ends 24 h after the NGM initial time (in this case, 29 January 0000 UTC). Figure 30 shows the magic chart for the second 12-h period based on the 1200 UTC 29 January model run.

Based on these two figures, and the 2 in per +20 NVD conversion, heavy snowfall could be expected across northern New England between 1200 UTC 29 January and 1200 UTC 30 January with 6-12 in during each 12-h period (3-6 in across northern Maine during the first 12 h).

There are several potential problems that forecasters must be aware of when using this procedure. First and foremost, this is model-based and only as good as the model. If the model warms the 850-mb temperatures too much, as it did in this case, the -3 to -5°C band could be displaced too far north. It also assumes a constant temperature for the entire period, based on the temperature at the beginning of the period. This is often erroneous, especially in systems that have one or more changeovers of precipitation type. The best use of the "magic chart," at least for this event, is to accept the model NVD field and modify the 850-mb thermal field to take into account other factors such as the track of the 850-mb low, evaporational cooling, cold air damming, and 850-mb thermal advection. In areas that remain all snow and have sufficient moisture to sustain continuous precipitation, this procedure will provide a good first guess of potential snowfall amounts.

During this event, heavy snow fell in the observed range from -2 to -10°C at 850 mb. Czepyha (1991) and Evenson (1992) presented case studies that showed how heavy snowfall can occur further into the cold air than predicted by the magic chart. Along the East Coast, an onshore flow advects Atlantic moisture inland, which can offset the magic chart -5°C criterion, supporting heavy snowfall at colder temperatures despite the limited amount of moisture that can be retained by the atmosphere at these temperatures. For this event, a strong onshore flow supplied abundant moisture to all of Maine and New Hampshire, well into the cold air.

In an attempt to determine how accurate this method was for this event, which lasted approximately 18 to 24 h, two 12-h periods of NVD were combined into a 24-h forecast ending at 1200 UTC 30 January (Fig. 31) and then compared to observed total snowfall (cf. Fig. 1). Overall, the 160-180 mb NVD across northern New England should have corresponded to 16-18 in of snow given favorable 850-mb forecast temperatures, and generally these amounts did verify. However, there were a few exceptions. One of the exceptions was in southern New Hampshire and coastal Maine, where ice pellets, freezing rain, and even some rain kept snow amounts down to a foot or less. Forecast 850-mb temperatures were warmer than -3°C for much of the 24-h period (Figs. 29 and 30) in this area; thus, the forecaster should not expect

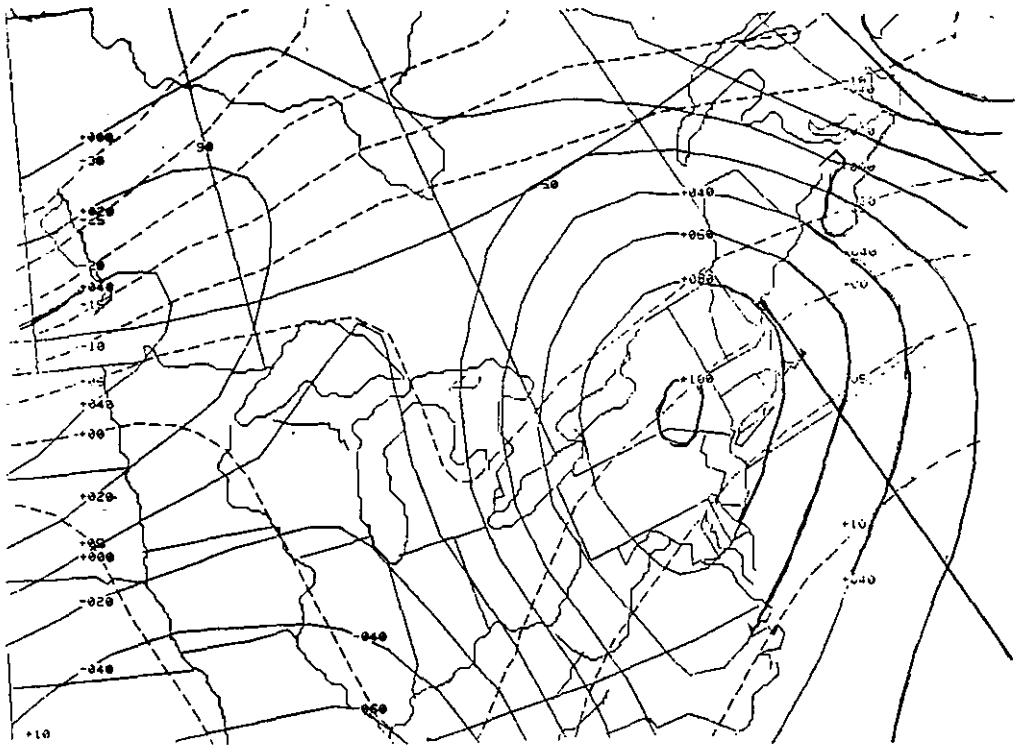

Figure 29. The "magic chart" from the 0000 UTC 29 January 1990 model run. Solid lines represent LFM-derived 700-mb NVD (12-24 h Net Vertical Displacement), and dashed lines represent 12-h NGM 850-mb isotherms.

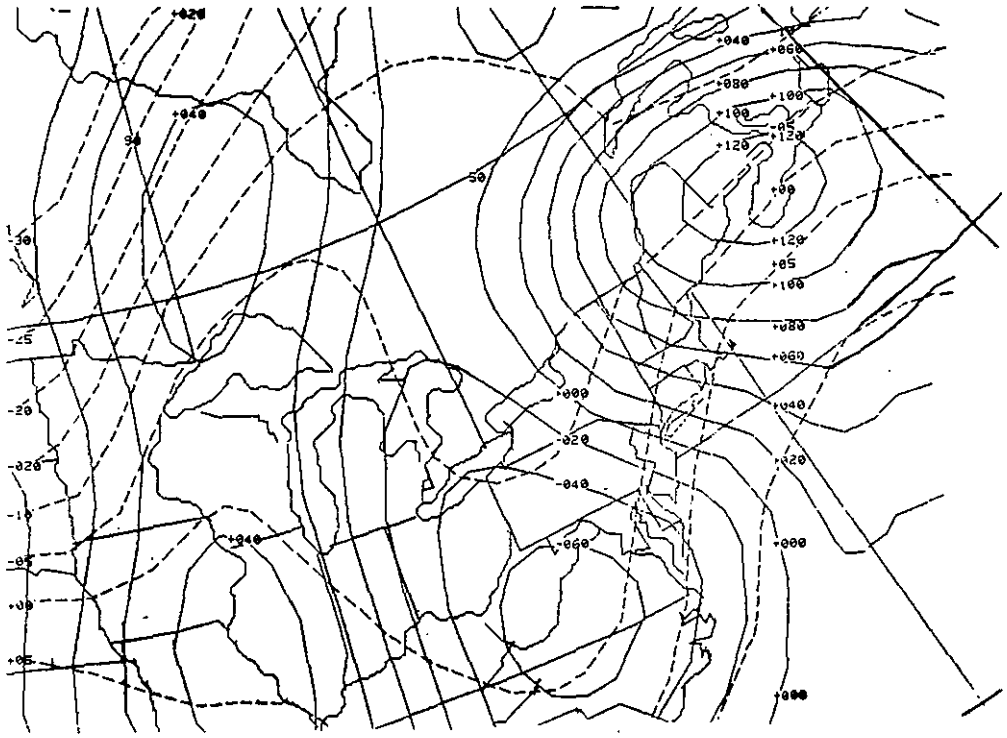

Figure 30. As in Figure 29, except from the 1200 UTC 29 January 1990 model run.

as much snow as indicated by the NVD values. Also, snowfall amounts up to 20 in fell on the windward (east) side of the White Mountains, while only 8-12 in fell on the leeward (west) side, due to the effects of orographic lifting and subsidence, respectively.

6. SOME EMPIRICAL RULES FOR WINTER STORMS

By applying some well known empirical rules of thumb, such as those developed by George (1960), it can be illustrated how synoptic-scale, dynamic numerical guidance can be tailored to local conditions. An understanding of local conditions and climatology can be better utilized to produce accurate and timely forecasts. Often, the busiest time for operational forecasters is also the most critical time to issue winter storm watches/warnings. Knowledge of empirical rules allow the forecaster to better utilize his or her time to produce the best forecast for a heavy snow event.

Several empirical rules used at WSFO Portland include: (1) snowfall is heaviest within the 700-mb closed contours; (2) the 850-mb 0°C isotherm through the 700-mb closed contour determines the boundary of snow versus rain, while the -2°C isotherm at 850 mb often marks the start of the moderate to heavy snow band; (3) the northern limit of snowfall is usually within 50 mi of the northernmost point of the last 700-mb closed contour; (4) the heavy snow band is about the same width as the distance between the 0 and -2°C isotherms at 850 mb; (5) the heavy snow will normally occur 100 to 200 mi to the left of the track of the 500-mb vorticity maximum; and (6) the LFM FOUS boundary layer potential temperature forecasts of 279 K represents the rain versus snow threshold. These rules have generally shown a high success rate in the northeastern United States.

During this storm, rules 1, 2, 3, and 5 corresponded closely to the observed distribution of heavy snow. By comparing initial analyses at 0000 UTC and 1200 UTC 30 January and 0000 UTC 31 January of 700-mb contours and 850-mb isotherms (Figs. 32, 33, 34), it can be seen how well rules 1, 2, and 3 worked together pointing to areas of heavy snowfall (in Fig. 32 an intermediate contour [not shown] would better depict the closed circulation around the low height center over Lake Erie).

Rule 4 was too conservative, as the heavy snow band extended well beyond the distance between the 0 and -2°C isotherms. This may be explained, in part, by evaporational cooling and strong warm air advection creating a tight thermal gradient, in addition to orographic influences enhancing snowfall amounts further inland. As for rule 6, the boundary-layer temperatures were forecast to remain at or below 279 K on both the 1200 UTC 29 January and 0000 UTC 30 January LFM runs for Maine and New Hampshire. However, this rule of thumb does not account for warming of a layer above the boundary layer, as happened at Portland (cf. Section 3C).

These empirical rules are just a few of the many tools that experienced forecasters apply to a particular event. They take little time to assess and in New England, in particular, they have been shown to be an effective indicator of a potential significant weather event, when viewed

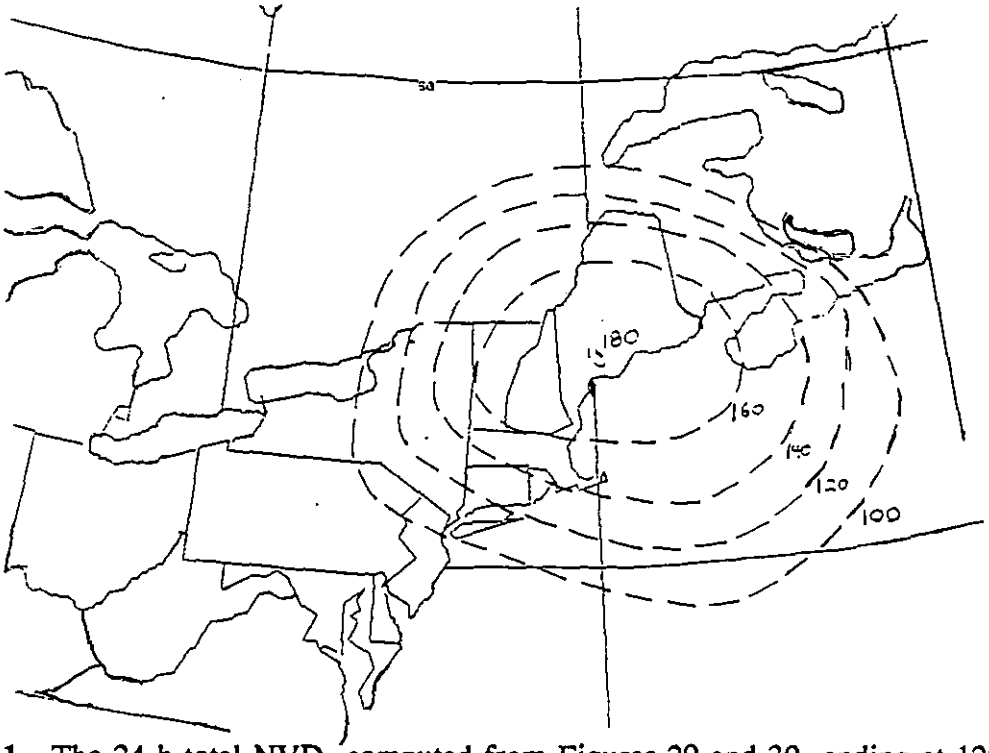

Figure 31. The 24-h total NVD, computed from Figures 29 and 30, ending at 1200 UTC 30 January 1990.

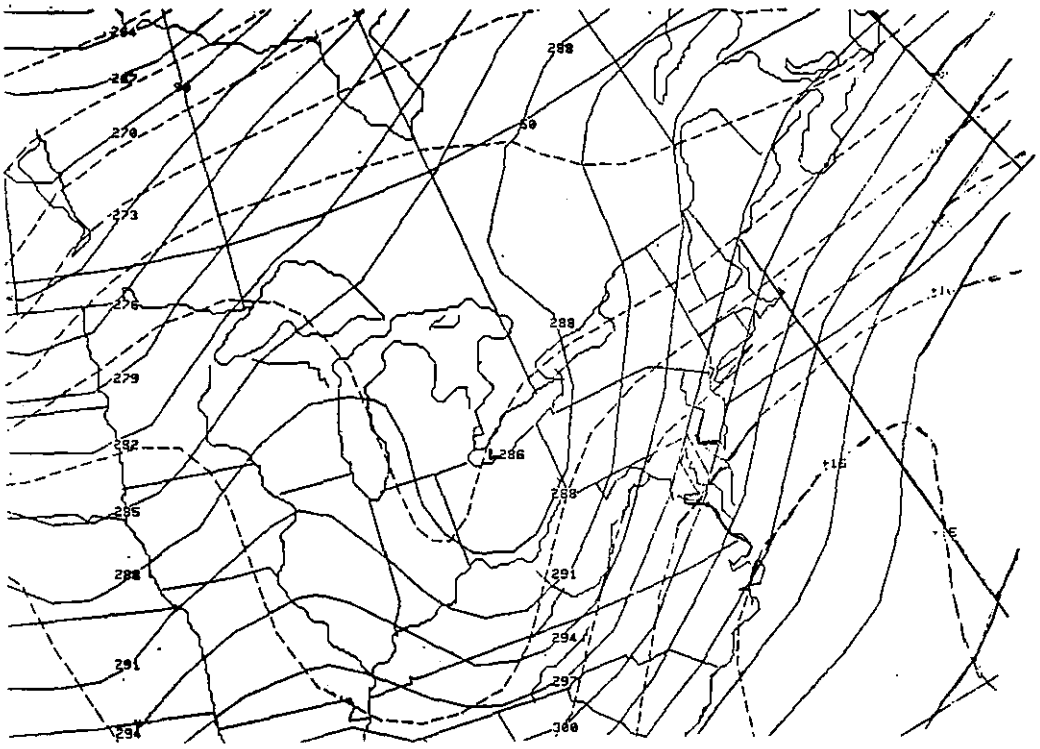

Figure 32. NMC 700-mb height (dm; solid lines) and 850-mb temperature (°C; dashed lines) analyses for 0000 UTC 30 January 1990.

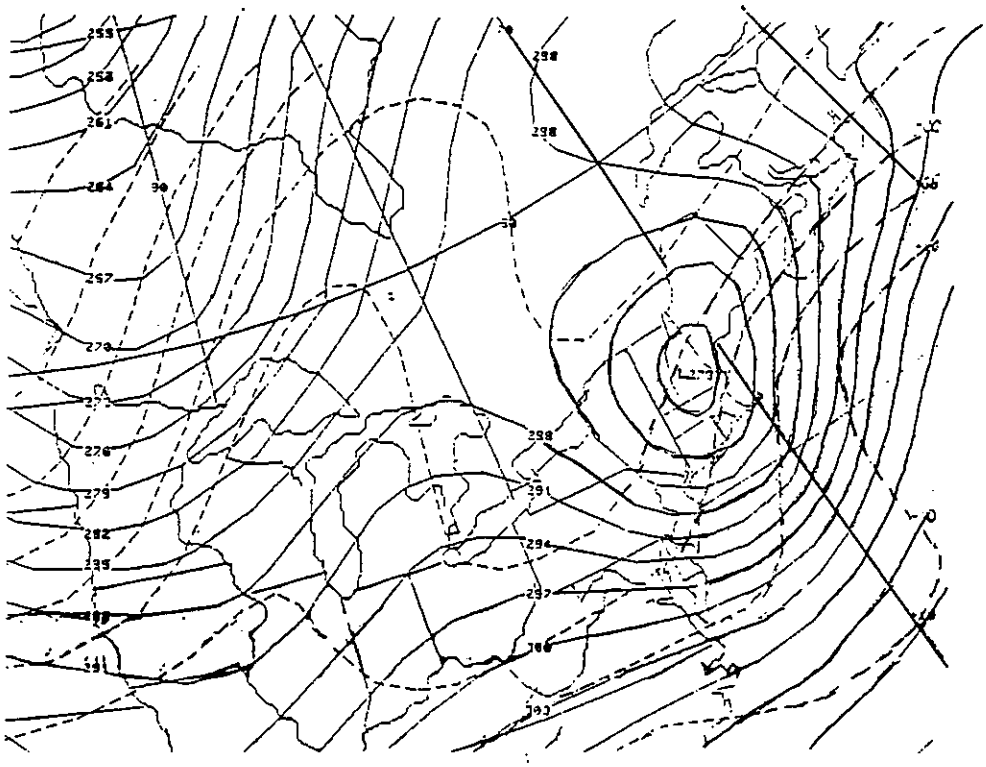

Figure 33. As in Figure 32, except for 1200 UTC 30 January 1990.

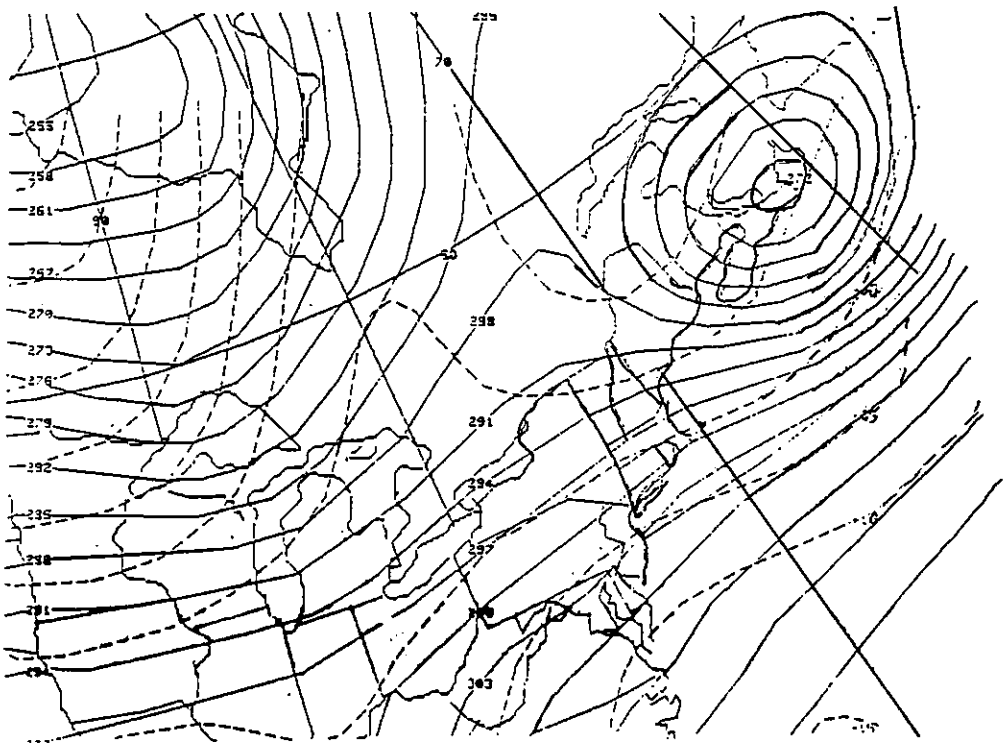

Figure 34. As in Figure 32, except for 0000 UTC 31 January 1990.

in the context of the overall synoptic situation.

7. FUTURE CONSIDERATIONS

High resolution data from the WSR-88D radar and vertical wind profilers should aid forecasters in detecting sub-synoptic-scale features, such as the development and movement of a coastal front, much sooner. WSR-88D base data (e.g., radial velocity) and derived products (e.g., Velocity Azimuth Display [VAD] winds) should help determine the strength of the low-level convergence along the coastal front. WSR-88D precipitation estimates will aid forecasters in determining precipitation rates for remote areas, and with its finer resolution and better sensitivity, the radar should be able to detect heavier mesoscale snowbands, as well as the full areal extent of the snow.

Wind profilers will provide forecasters with a high frequency, three-dimensional cross section of the troposphere that will enable forecasters to observe developing or changing features above the ground. Layers of warm and cold air advection, descending jets, the depth of cold air damming, and low-level jets will be easier to detect than with the current, twice-a-day rawinsonde observations.

The WSR-88D radar and wind profilers will be extremely useful in providing real-time, mesoscale data needed to analyze the small-scale features that often have a significant effect on the synoptic-scale event.

8. CONCLUSIONS

In order to forecast winter storm events in the northeastern United States, operational forecasters need to examine the important synoptic and mesoscale features, such as coastal fronts; account for local effects, such as orography; and apply time-tested forecast techniques and empirical rules. This requires supplementing standard NMC guidance. Data analyses, such as computing sounding wet bulb temperatures, are very important. Many software applications can be run on local computer systems that can help forecasters prepare meso-analyses, produce statistical prognoses (e.g., precipitation types), and prepare special charts based upon standard NMC guidance (e.g., the "magic chart"). The winter storm of 29-30 January 1990 is an excellent example of how the operational forecaster can combine the use of NMC guidance with local applications software, techniques, and rules of thumb to produce a better forecast.

REFERENCES

Auciello, E. P., 1989: A method for predicting meteorological bombs in the western North Atlantic Ocean. *Postprints, Second National Winter Weather Workshop*, Raleigh, *NOAA Technical Memorandum* NWS ER-82, U.S. Department of Commerce, 209-217. [NTIS PB90-147414/AS]

Bosart, L. F., 1975: New England coastal frontogenesis. *Quart. J. Roy. Meteor. Soc.*, **101**, 957-978.

_____, C. J. Vaudo, and J. H. Helsdon, Jr., 1972: Coastal frontogenesis. *J. of Appl. Meteor.*, **11**, 1236-1258.

Capriola, S. J., 1990: A local verification of LFM and NGM quantitative precipitation forecasts for Maine and New Hampshire. *Eastern Region Technical Attachment* No. 90-6C, National Weather Service, NOAA, U.S. Department of Commerce, 4 pp. [Available from NWS Eastern Region Scientific Services Division, Bohemia, NY.]

Carr, F. H., 1988: Introduction to numerical weather prediction models at the National Meteorological Center. Univ. of Oklahoma School of Meteor., 63 pp. [Available from NWS Southern Region Scientific Services Division, Fort Worth, TX.]

Chaston, P. R., 1989: The magic chart for forecasting snow amounts. *Natl. Wea. Dig.*, **14**(1), 20-22.

Czepyha, L., 1991: Heavy snowfall over the Southeast Atlantic Coast on December 22-24, 1989. *Eastern Region Technical Attachment* No. 91-7A, National Weather Service, NOAA, U.S. Department of Commerce, 4 pp. [Available from NWS Eastern Region Scientific Services Division, Bohemia, NY.]

Evenson, E. C., 1992: A case study involving local effects that influence the application of the magic chart. *Preprints, Symp. on Wea. Forecasting*, Atlanta, Amer. Meteor. Soc., 142-147.

George, J. J., 1960: *Weather Forecasting for Aeronautics*. Academic Press, New York, 673 pp.

Gilhousen, D. B., 1991: Documentation of real-time quality control checks for moored and headland stations, 5 pp. [Unpublished report available from National Data Buoy Center, Stennis Space Center, MS.]

Hart, J. A., and J. Korotky, 1991: The SHARP workstation v1.50 user's manual. National Weather Service, NOAA, U.S. Department of Commerce, 30 pp. [Available from NWS Eastern Region Scientific Services Division, Bohemia, NY.]

Jensenius, Jr., J. S., 1989: A statistical comparison of the forecasts produced by the NGM and LFM for the cool season of 1987-1988. *TDL Office Note* 89-4, National Weather Service, NOAA, U.S. Department of Commerce, 14 pp. [Available from Techniques Development Laboratory, Silver Spring, MD.]

Junker, N. W., J. E. Hoke, and R. H. Grumm, 1989: Performance of NMC's regional models. *Wea. Forecasting*, **4**, 368-390.

Kocin, P. J., and L. W. Uccellini, 1990: *Snowstorms Along the Northeastern Coast of the United States: 1955 to 1985*. Amer. Meteor. Soc., Boston, 280 pp.

_____, _____, R. H. Grumm, and W. C. Skillman, 1989: Jet streak circulations associated with a moderate snowfall event as diagnosed from NGM model output. *Preprints, 12th Conf. on Wea. Analysis and Forecasting*, Monterey, Amer. Meteor. Soc., 292-297.

Marks, F. D., and P. M. Austin, 1979: Effects of the New England coastal front on the distribution of precipitation. *Mon. Wea. Rev.*, **107**, 53-67.

McCarthy, D. H., 1977: A study of the vertical structure of the New England coastal front. M.S. thesis, Univ. of Wisconsin, Madison, 82 pp.

Nielsen, J. W., 1989: The formation of New England coastal fronts. *Mon. Wea. Rev.*, **117**, 1380-1401.

Ronco, Jr., J. A., 1988: A procedure for forecasting precipitation type using NGM low level temperatures and LFM MOS frozen precipitation probabilities. *Eastern Region Technical Attachment* No. 88-2, National Weather Service, NOAA, U.S. Department of Commerce, 6 pp. [Available from NWS Eastern Region Scientific Services Division, Bohemia, NY.]

Sanders, F., and E. P. Auciello, 1989: Skill in prediction of explosive cyclogenesis over the western North Atlantic Ocean, 1987/88: A forecast checklist and NMC dynamical models. *Wea. Forecasting*, **4**, 157-172.

_____, and J. Gyakum, 1980: Synoptic-dynamic climatology of the bomb. *Mon. Wea. Rev.*, **108**, 1589-1606.

Uccellini, L. W., and P. J. Kocin, 1987: An examination of vertical circulations associated with heavy snow events along the East Coast of the United States. *Wea. Forecasting*, **2**, 289-308.

NWS ER 46 An Objective Method of Forecasting Summertime Thunderstorms. John F. Townsend and Russell J. Younkin. May 1972. (COM-72-10765)

NWS ER 47 An Objective Method of Preparing Cloud Cover Forecasts. James R. Sims. August 1972. (COM-72-11382)

NWS ER 48 Accuracy of Automated Temperature Forecasts for Philadelphia as Related to Sky Condition and Wind Direction. Robert B. Wassall. September 1972. (COM-72-11473)

NWS ER 49 A Procedure for Improving National Meteorological Center Objective Precipitation Forecasts. Joseph A. Ronco, Jr. November 1972. (COM-73-10132)

NWS ER 50 PEATMOS Probability of Precipitation Forecasts as an Aid in Predicting Precipitation Amounts. Stanley E. Wasserman. December 1972. (COM-73-10243)

NWS ER 51 Frequency and Intensity of Freezing Rain/Drizzle in Ohio. Marvin E. Miller. February 1973. (COM-73-10570)

NWS ER 52 Forecast and Warning Utilization of Radar Remote Facsimile Data. Robert E. Hamilton. July 1973. (COM-73-11275)

NWS ER 53 Summary of 1969 and 1970 Public Severe Thunderstorm and Tornado Watches Within the National Weather Service Eastern Region. Marvin E. Miller and Lewis H. Ramey. October 1973. (COM-74-10160)

NWS ER 54 A Procedure for Improving National Meteorological Center Objective Precipitation Forecasts - Winter Season. Joseph A. Ronco, Jr. November 1973. (COM-74-10200)

NWS ER 55 Cause and Prediction of Beach Erosion. Stanley E. Wasserman and David B. Gilhousen. December 1973. (COM-74-10036)

NWS ER 56 Biometeorological Factors Affecting the Development and Spread of Planet Diseases. V. J. Villi. July 1974. (COM-74-11625/AS)

NWS ER 57 Heavy Fall and Winter Rain In The Carolina Mountains. David B. Gilhousen. October 1974. (COM-74-11761/AS)

NWS ER 58 An Analysis of Forecasters' Propensities In Maximum/Minimum Temperature Forecasts II. Randy Racer. November 1974. COM-75-10063/AS)

NWS ER 59 Digital Radar Data and its Application in Flash Flood Potential. David D. Sisk. March 1975. (COM-75-10582/AS)

NWS ER 60 Use of Radar Information in Determining Flash Flood Potential. Stanley E. Wasserman. December 1975. (PB250071/AS)

NWS ER 61 Improving Short-Range Precipitation Guidance During the Summer Months. David B. Gilhousen. March 1976. (PB256427)

NWS ER 62 Locally Heavy Snow Downwind from Cooling Towers. Reese E. Otts. December 1976. (PB263390/AS)

NWS ER 63 Snow in West Virginia. Marvin E. Miller. January 1977. (PB265419/AS)

NWS ER 64 Wind Forecasting for the Monongahela National Forest. Donald E. Risher. August 1977. (PB272138/AS)

NWS ER 65 A Procedure for Spraying Spruce Budworms in Maine during Stable Wind Conditions. Monte Glovinsky. May 1980. (PB80-203243)

NWS ER 66 Contributing Factors to the 1980-81 Water Supply Drought, Northeast U.S. Solomon G. Summer. June 1981. (PB82-172974)

NWS ER 67 A Computer Calculation and Display System for SLOSH Hurricane Surge Model Data. John F. Townsend. May 1984. (PB84-198753)

NWS ER 68 A Comparison Among Various Thermodynamic Parameters for the Prediction of Convective Activity. Hugh M. Stone. April 1985. (PB85-206217/AS)

NWS ER 69 A Comparison Among Various Thermodynamic Parameters for the Prediction of Convective Activity, Part II. Hugh M. Stone. December 1985. (PB86-142353/AS)

NWS ER 70 Hurricane Gloria's Potential Storm Surge. Anthony G. Gigi and David A. Wert. July 1986. (PB86-226644/AS)

NWS ER 71 Washington Metropolitan Wind Study 1981-1986. Clarence Burke, Jr. and Carl C. Ewald. February 1987. (PB87-151908/AS)

NWS ER 72 Mesoscale Forecasting Topics. Hugh M. Stone. March 1987. (PB87-180246/AS)

NWS ER 73 A Procedure for Improving First Period Model Output Statistics Precipitation Forecasts. Antonio J. Lacroix and Joseph A. Ronco, Jr. April 1987. (PB87-180238/AS)

NWS ER 74 The Climatology of Lake Erie's South Shoreline. John Kwiatkowski. June 1987. (PB87-205514/AS)

NWS ER 75 Wind Shear as a Predictor of Severe Weather for the Eastern United States. Hugh M. Stone. January 1988. (PB88-157144)

NWS ER 76 Is There A Temperature Relationship Between Autumn and the Following Winter? Anthony Gigi. February 1988. (PB88-173224)

NWS ER 77 River Stage Data for South Carolina. Clara Cillentine. April 1988. (PB88-201991/AS)

NWS ER 78 National Weather Service Philadelphia Forecast Office 1987 NOAA Weather Radio Survey & Questionnaire. Robert P. Wanton. October 1988. (PB89-111785/AS)

NWS ER 79 An Examination of NGM Low Level Temperature. Joseph A. Ronco, Jr. November 1988. (PB89-122543/AS)

NWS ER 80 Relationship of Wind Shear, Buoyancy, and Radar Tops to Severe Weather 1988. Hugh M. Stone. November 1988. (PB89-1222419/AS)

NWS ER 81 Relation of Wind Field and Buoyancy to Rainfall Inferred from Radar. Hugh M. Stone. April 1989. (PB89-208326/AS)

NWS ER 82 Second National Winter Weather Workshop, 26-30 Sept. 1988. Postprints. Laurence G. Lee. June 1989. (PB90-147414/AS)

NWS ER 83 A Historical Account of Tropical Cyclones that Have Impacted North Carolina Since 1586. James D. Stevenson. July 1990. (PB90-259201)

NWS ER 84 A Seasonal Analysis of the Performance of the Probability of Precipitation Type Guidance System. George J. Maglaras and Barry S. Goldsmith. September 1990. (PB93-160802)

NWS ER 85 The Use of ADAP to Examine Warm and Quasi-Stationary Frontal Events in the Northeastern United States. David R. Vallee. July 1991. (PB91-225037)

NWS ER 86 Rhode Island Hurricanes and Tropical Storms A Fifty-Six Year Summary 1936-0991. David R. Vallee. March 1993. (PB93-162006)

NWS ER 87 Post-print Volume, Third National Heavy Precipitation Workshop, 16-20 Nov. 1992. April 1993. (PB93-186625)

NWS ER 88 A Synoptic and Mesoscale Examination of the Northern New England Winter Storm of 29-30 January 1990. Robert A. Marine and Steven J. Capriola. July 1994.

NOAA SCIENTIFIC AND TECHNICAL PUBLICATIONS

The National Oceanic and Atmospheric Administration was established as part of the Department of Commerce on October 3, 1970. The mission responsibilities of NOAA are to assess the socioeconomic impact of natural and technological changes in the environment and to monitor and predict the state of the solid Earth, the oceans and their living resources, the atmosphere, and the space environment of the Earth.

The major components of NOAA regularly produce various types of scientific and technical information in the following kinds of publications:

PROFESSIONAL PAPERS—Important definitive research results, major techniques, and special investigations.

CONTRACT AND GRANT REPORTS—Reports prepared by contractors or grantees under NOAA sponsorship.

ATLAS—Presentation of analyzed data generally in the form of maps showing distribution of rainfall, chemical and physical conditions of oceans and atmosphere, distribution of fishes and marine mammals, ionospheric conditions, etc.

TECHNICAL SERVICE PUBLICATIONS—Reports containing data, observations, instructions, etc. A partial listing includes data serials; prediction and outlook periodicals; technical manuals, training papers, planning reports, and information serials; and miscellaneous technical publications.

TECHNICAL REPORTS—Journal quality with extensive details, mathematical developments, or data listings.

TECHNICAL MEMORANDUMS—Reports of preliminary, partial, or negative research or technology results, interim instructions, and the like.

Information on availability of NOAA publications can be obtained from:

NATIONAL TECHNICAL INFORMATION SERVICE
U.S. DEPARTMENT OF COMMERCE
5285 PORT ROYAL ROAD
SPRINGFIELD, VA 22161